ESD-TDR-64-365

Group Report 1964-6

Random Noise Considerations in the Design of Magnetic Film Sense Amplifiers

H. Blatt

17 August 1964

Prepared under Electronic Systems Division Contract AF 19(628)-500 by

Lincoln Laboratory
MASSACHUSETTS INSTITUTE OF TECHNOLOGY
Lexington, Massachusetts

The work reported in this document was performed at Lincoln Laboratory, a center for research operated by Massachusetts Institute of Technology, with the support of the U.S. Air Force under Contract AF 19(628)-500.

MASSACHUSETTS INSTITUTE OF TECHNOLOGY

LINCOLN LABORATORY

RANDOM NOISE CONSIDERATIONS IN THE DESIGN OF MAGNETIC FILM SENSE AMPLIFIERS

H. BLATT

Group 23

GROUP REPORT 1964-6

17 AUGUST 1964

LEXINGTON MASSACHUSETTS

ABSTRACT

A model of a magnetic film sense system is presented. Using the model the mean time between false readouts due to random noise is determined as a function of the system parameters; total magnetic flux switched, switching time, sense line resistance, amplifier noise factor and linear amplifier filter efficiency. (The filter efficiency with respect to a given input pulse shape is the signal-to-noise ratio at the output of the amplifier divided by the corresponding signal-to-noise ratio at the output of a filter matched to the pulse shape.) The degradation of signal-to-noise ratio caused by introduction of a quick recovery "short" time constant is determined and shown experimentally.

Accepted for the Air Force
Franklin C. Hudson, Deputy Chief
Air Force Lincoln Laboratory Office

TABLE OF CONTENTS

ACKNOWLEDGEMENT

The author wishes to acknowledge the interest and helpful comments of the members of Group 23, expecially Dr. D. J. Eckl for his many suggestions concerning Sections 2 and 3, and J. I. Raffel for his interest and encouragement in the project.

I. INTRODUCTION

As film elements and therefore signals become smaller, the corrupting influence of the random noise processes which accompany the sensing operation become more significant. Even with film elements in present use, noise significantly reduces operating margins.[9] Further reduction in element size will certainly result in noise becoming a first-order problem.[1, 2] Power gain and bandwidth requirements now dictate the use of multistage sense amplifiers and the use of smaller elements will require even greater amplifier bandwidths and perhaps more stages. It is reasonable to assume that the overall bandwidth of such amplifiers has only a weak dependence on any one stage. If that is the case, we may consider an n-stage amplifier as being an essentially distortionless but noisy first stage cascaded with a n-1 stage linear filter-amplifier. If we restrict our attention to amplifiers not designed to pass very low frequencies, the noise output of the first stage may be considered white, i.e., noise power uniformly distributed over all frequencies. Since there are no first stage bandwidth restrictions in our model, we must consider the first stage noise power per cycle of bandwidth so the signal-to-noise ratio associated with the first stage is an energy ratio. The signal-to-noise ratio of the entire amplifier, the measure which we eventually wish to maximize, is a power ratio and is related to the first stage signal-to-noise ratio through the filter characteristics of the n-1

stage amplifier following the input stage. The problem thus breaks down into two separate problems: 1) maximizing the first stage signal-to-noise energy ratio principally through proper choice of amplifier configuration, emitter current and source resistance, and 2) maximizing the filter-amplifier output signal-to-noise power ratio for a given signal-to-noise energy ratio into the filter by the proper choice of filter characteristics. The filter design depends on the signal waveform whereas the input stage design does not. Sections 2 and 3 of this report are concerned with the first problem and Section 4 with the second.

2. SOURCES OF TRANSISTOR NOISE

2.1 Frequency Range of Interest

The noise processes in transistors fall into two categories. The first includes those which are characterized by the shot effect and have flat power spectra over a wide band of frequencies. The noise processes dealt with in this paper are in this category. The second category includes processes which predominate at low frequencies and have approximately a 1/f power spectrum. These are variously described as 1/f noise or "excess noise." In modern junction transistors the noise power due to these processes becomes negligible compared with the shot noise above the lower audio frequencies.[3] Since 1/f noise will not be discussed, the results obtained do not apply to amplifiers designed to pass very low frequencies (see Fig. 1). A

further limitation on the range of validity of the results is the assumption that the high frequency behavior of the entire amplifier is not governed by the high frequency behavior of the current gain of the first stage alone – a reasonable assumption for a multistage amplifier.

2.2 The Beatie Shot Noise Model[4]

A number of transistor shot noise models have been proposed which show reasonable agreement with experiment.[5, 6, 7] The calculations in this paper are based on Beatie's shot noise model which requires four uncorrelated sources of noise. Three of the sources are associated with transistor action proper and the fourth with the base spreading resistance r_b'. Although other models have the advantage of requiring fewer sources, these are partially correlated statistically so that output noise calculations become more difficult. The three intrinsic noise sources of the Beatie model are represented as current sources and are associated with generation-recombination near the emitter, generation-recombination near the collector and with the diffusion process itself. These sources are shown super-imposed on the Giacolleto common emitter transistor equivalent circuit in Fig. 2.[6] Each of the intrinsic noise current sources shows shot effect and has a mean square value proportional to the product of the bandwidth and a d-c current.

$$\overline{i_{ne}^2} = 2q\,\Delta f\,Ie\,(1 - \alpha_n) \qquad amp^2 \qquad (1)$$

$$\overline{i_{nd}^2} = 2q\,\Delta f\,Ie\,\alpha_n \qquad amp^2 \qquad (2)$$

$$\overline{i_{nc}^2} = 2q\,\Delta f\,Ico\,\gamma \qquad amp^2 \qquad (3)$$

where α_n and α_I refer to the normal (emitter-to-collector) and inverted (collector-to-emitter) current gain, q is the electronic charge, Δf is the bandwidth, Ie is the d-c emitter current and $\gamma = \frac{1 - \alpha_I}{1 - \alpha_n \alpha_I}$. The mean square values of the thermal noise sources are given by the Nyquist formula:

$$\overline{e_{nb}^2} = 4kT\,\Delta f\,r_b' \qquad volt^2 \qquad (4)$$

$$\overline{e_{ns}^2} = 4kT\,\Delta f\,Rs \qquad volt^2 \qquad (5)$$

where k is Boltzman's constant and T is the absolute temperature.

Following Peterson,[6] we transform each noise source to the output through the gain mechanism of the transistor and obtain the

following relations where the subscript N denoting output quantity has replaced n.

$$\overline{i_{Ne}^2} = \frac{\alpha^2}{(1-\alpha)} \cdot \frac{2\ Ie\ q\ \Delta f\ (Rs + r_b')^2}{(Rs + r_b' + \frac{re}{1-\alpha})^2} \quad amp^2 \qquad (6)$$

$$\overline{i_{Nc}^2} = \frac{1}{(1-\alpha)^2} \cdot \frac{2\gamma\ Ico\ q\ \Delta f\ (Rs + r_b' + re)^2}{(Rs + r_b' + \frac{re}{1-\alpha})^2} \quad amp^2 \qquad (7)$$

$$\overline{i_{Nd}^2} = 2\ \alpha\ Ie\ q\ \Delta f \quad amp^2 \qquad (8)$$

$$\overline{i_{Nb}^2} = \frac{\alpha^2}{(1-\alpha)^2} \cdot \frac{4kT\ r_b'\ \Delta f}{(Rs + r_b' + \frac{re}{1-\alpha})^2} \quad amp^2 \qquad (9)$$

$$\overline{i_{Ns}^2} = \frac{\alpha^2}{(1-\alpha)^2} \cdot \frac{4kT\ Rs\ \Delta f}{(Rs + r_b' + \frac{re}{1-\alpha})^2} \quad amp^2 \qquad (10)$$

where $re = \frac{k\ T}{q\ Ie}$

α = normal current gain

These five quantities represent the mean square value of the output (collector) currents due to the five sources of noise. The expressions for the output noise components may be simplified somewhat

by substituting $\beta = \frac{\alpha}{1-\alpha} \approx \frac{1}{1-\alpha}$ and $\gamma \approx 1$ in the above formulas and using the numerical values for q, T, and k. We then have for the noise components on a <u>per cycle</u> basis:

$$\overline{i_{Ne}^2} = 3.2 \times 10^{-19} \frac{\beta\,(Rs + r_b')^2\, Ie}{(Rs + r_b' + \beta re)^2} \quad amp^2 \qquad (11)$$

$$\overline{i_{Nc}^2} = 3.2 \times 10^{-19} \frac{\beta^2 (Rs + r_b' + re)^2\, Ico}{(Rs + r_b' + \beta re)^2} \quad amp^2 \qquad (12)$$

$$\overline{i_{Nd}^2} = 3.2 \times 10^{-19}\, Ie \quad amp^2 \qquad (13)$$

$$\overline{i_{Nb}^2} = 1.65 \times 10^{-20} \frac{\beta^2\, r_b'}{(Rs + r_b' + \beta re)^2} \quad amp^2 \qquad (14)$$

$$\overline{i_{Ns}^2} = 1.65 \times 10^{-20} \frac{\beta^2\, Rs}{(Rs + r_b' + \beta re)^2} \quad amp^2 \qquad (15)$$

The total output mean square noise current $\overline{i_N^2}$ may be obtained by simply adding the noise components since the components are statistically uncorrelated. The noise components are seen to be strong functions of Ie, r_b', Rs, β, Ico (and temperature, T). The

relative importance of each of the five terms depends on the quiescent operating conditions. In particular, for a given transistor, at a given temperature, the noise performance depends on the emitter current Ie and the source resistance Rs. However, in order to get a feeling for the relative importance of each term, it will be helpful to assume for the present an operating condition such that Rs $\ll r_b'$ so that Rs may be left out of the calculations. This will turn out to be a poor choice of source resistance for good signal-to-noise ratio, but the inclusion of calculations based on this assumption are justified (other than for simplification) on the grounds that many magnetic film sense amplifiers are operated in such a (noisy) fashion.[8, 9] The calculations of Sections 2.3 and 2.4 below are based on this assumption.

2.3 Variation of Noise Components with Current Gain β

Of the five terms contributing to output noise, we have to consider only the terms $\overline{i_{Ne}^2}$, $\overline{i_{Nd}^2}$, $\overline{i_{Nb}^2}$. The term due to Rs is negligible by assumption and the Ico term is negligible compared with the others over the emitter current ranges studied ($> 100\ \mu a$) i.e., $Ie \gg \beta Ico$. This would be true of any good quality transistor used in a low noise application. The three remaining terms are tabulated below:

$$\overline{i_{Ne}^2} = \frac{3.2 \times 10^{-19}\ \beta\ (r_b')^2\ Ie}{(r_b' + \beta re)^2} \qquad amp^2 \qquad (16)$$

$$\overline{i_{Nb}^2} = \frac{1.65 \times 10^{-20}\ \beta^2\ r_b'}{(r_b' + \beta re)^2} \qquad amp^2 \qquad (17)$$

$$\overline{i_{Nd}^2} = 3.2 \times 10^{-19}\ Ie \qquad amp^2 \qquad (18)$$

These three components together with their sum are plotted in Fig. 3 as a function of β for Ie=5 ma and r_b' = 100 ohms. The term responsible for the increase in output noise with increasing β is the term associated with the thermal noise of r_b'. In this connection, we may think of r_b' as a source delivering power to the intrinsic transistor whose input resistance is βre. The thermal power input to the intrinsic transistor is $\frac{(4kT\ r_b')\ \beta re}{(r_b' + \beta re)^2}$. The maximum thermal power that r_b' can deliver to the input is kT and the maximum power transfer occurs for $\beta re = r_b'$; i.e., for $\beta = \frac{r_b'}{re}$ if power transfer is regarded as a function of β. The power gain* of the intrinsic transistor is $\beta \frac{R\ \ell}{re}$ so that while the thermal power

---

* The power gain of a transducer is the ratio of the power delivered to the load by the transducer to the power input to the transducer. Transducer gain is the ratio of the power delivered by the transducer to the load to the power available from the source.

delivered to the input falls off as $\frac{1}{\beta}$ for $\beta \gg \frac{r_b'}{re}$ the power gain increases as β with the result that the noise power output due to r_b' levels off for high β. Data showing increasing output noise power for 18 T2217** transistors of varying current gains is shown in Fig. 4.

2.4 Variation of Noise Components with Emitter Current

In this section we consider the variation of the output noise components for a given transistor as a function of emitter current. We still need only consider the components of the previous section (equations 16 through 18). These equations may be further simplified if $\beta re \gg r_b'$ over the range of emitter currents of interest. The T2217 transistors used in this study have β's (at 5 ma) of 160 which correspond to the median β of a test group of 1000. The current gain of three randomly chosen T2217's was measured as a function of emitter current. The results are shown in Fig. 5. From 100 μa to 5 ma β varied from 50 to 160 so that βre varied from 10K to 820 ohms, thus for these or similar transistors over this range $\beta re \gg r_b'$. At higher currents (> 10 ma) there is less justification for the approximation. The simplified equations for the noise components are:

** A limited production MADT similar to the 2N769.

$$\overline{i_{Nd}^2} = 3.2 \times 10^{-19}\ Ie \qquad amp^2 \qquad (19)$$

$$\overline{i_{Nb}^2} = \frac{1.65 \times 10^{-20}\ \beta^2\ r_b'^2}{(r_b' + \beta re)^2} \approx \frac{1.65 \times 10^{-20}\ r_b'^2}{re^2} = \qquad (20)$$

$$1.65 \times 10^{-20} \frac{r_b'^2}{\left(\frac{kT}{qIe}\right)^2} = 2.5 \times 10^{-17}\ r_b'^2\ Ie^2$$

$$\overline{i_{Ne}^2} = \frac{3.2 \times 10^{-19}\ \beta\ r_b'^2\ Ie}{(r_b' + \beta re)^2} \approx \frac{3.2 \times 10^{-19}\ r_b'^2\ Ie}{\beta(re)^2} = \qquad (21)$$

$$\frac{3.2 \times 10^{-19}\ r_b'^2\ Ie}{\beta \left(\frac{kT}{qIe}\right)^2} = 4.73 \times 10^{-16} \frac{r_b'^2}{\beta}\ Ie^3 .$$

The simplified components are plotted in Fig. 6 together with their sum. Also plotted for comparison is the total mean square collector noise current (per cycle) obtained from wide-band measurements (10 KC to 3 MC) made on a T2217 transistor (#836). The value for r_b' used in the calculations, 75 ohms, is the value determined by an independent measurement of #836*. Similarly, the current gain in the calculations is the current gain of #836. At low currents

---

* The input resistance at 1 mc was measured and βre subtracted from the measured value.

($< 200\ \mu a$) the total output noise power is governed by the diffusion term $\overline{i_{Nd}^2}$ and has a first power dependence on Ie. At higher currents the dominant noise component is that due to the amplified thermal noise of r_b' which varies as Ie^2. At still higher currents (> 30 ma) where measurements were not made, the simplified model predicts a cubic dependence on Ie but at 30 ma $\beta re \approx r_b'$ so the simplifying assumption breaks down.

3. DESIGN OF INPUT STAGE FOR MAXIMUM SIGNAL-TO-NOISE RATIO

3.1 Signal-to-Noise Ratio and Noise Factor

In general, the source resistance Rs is not negligible compared with r_b'. Part of the output noise is then due to the (amplified) thermal noise of the source and part is due to the noise sources within the transistor itself which nevertheless is affected by Rs (Section 2.2). It is useful to have a measure which indicates the fraction of the total output noise power due to noise sources within the transistor. The average Noise Factor $\overline{F}$, or its logarithmic equivalent the average noise figure (average noise figure = $10 \log_{10} \overline{F}$) is such a measure. The average noise factor of a transducer is defined as the ratio of (1) the total noise power delivered into the output termination by the transducer at all frequencies to (2) that portion of (1) engendered by the input termination (at standard temperature).[10] If P_s is the output noise

power due to the source termination, and P_T is the output noise power due to the internal noise sources (which depends on the source termination Rs), then:

$$\overline{F} = \frac{P_s + P_T}{P_s} = 1 + \frac{P_T}{P_s} \tag{22}$$

It can be shown that $\overline{F}$ has a minimum with respect to the source resistance Rs. Strictly speaking, it can be shown that F the noise factor at a single frequency [i.e., narrow band of frequencies] has a minimum with respect to Rs. But since our model assumes a flat-noise power spectrum for the input stage, $F = \overline{F}$ within the band of interest.

An alternative but equivalent definition of average noise factor is:

$$\overline{F} = \frac{\text{Signal-to-noise ratio at input}}{\text{Signal-to-noise ratio at output}} \tag{23}$$

where input signal-to-noise ratio is the available signal-to-noise ratio of the source. i.e.,

$$\text{input signal-to-noise energy ratio} = \frac{\int \frac{e_s^2}{4\,Rs}\,dt}{kT} \quad * \tag{24}$$

So that we have using equation 23

$$\overline{F} = \frac{\int \frac{e_s^2}{4\,Rs}\,dt}{kT} \cdot \left[\frac{1}{\text{output signal-to-noise ratio}}\right] \tag{25}$$

$$\therefore \quad \text{output signal-to-noise ratio} \equiv E/N_o = \frac{\int e_s^2\,dt}{4\,Rs\,kT\,\overline{F}} \tag{26}$$

---

* Since the bandwidth is not restricted at this point in the amplifier, the signal energy and noise energy, (power per cycle) must be used. The ratio E/N_o is an energy ratio.

If a transformer with turns ratio 1:a (Fig. 7) is inserted between source and transistor, the output signal-to-noise ratio becomes:

$$E/N_o = \frac{\int e_s^2 \, dt}{4 \, r_s \, kT \, \overline{F}} \qquad (27)$$

where the average noise factor $\overline{F}$ depends on the transformed source resistance $Rs = a^2 r_s$ while the available input signal-to-noise ratio depends on the actual source resistance r_s. Thus, to maximize E/N_o one requires the lowest possible source resistance and a transformer to transform this low resistance to the resistance which minimizes $\overline{F}$. For an electrically short unterminated sense line r_s = total line resistance. For an electrically long line terminated at the far end in its characteristic impedance $r_s = Z_o$. The inverse relationship between r_s and E/N_o simply reflects the fact that as the actual source resistance is made lower, more signal power may be extracted from it before its noise becomes comparable to the amplifier noise. The average Noise Factor for a T2217 with resistive input termination was measured as a function of Rs and Ie over the frequency range 10 Kc to 3.5 mc (Fig. 8). The curves show broad minima with respect to both Rs and Ie.

3.2 Choice of Input Stage Configuration

In a multistage amplifier significant noise may be contributed to the output by stages succeeding the first. The noise factor of the entire amplifier is given by Friis' formula[11]

$$F = F_1 + \frac{F_2 - 1}{G_1} + \frac{F_3 - 1}{G_1 G_2} + \ldots \qquad (28)$$

where F_1 is noise factor of first stage

F_2 is noise factor of second stage, etc.

G_1 is available gain of first stage*

G_2 is available gain of second stage, etc.

So that the second stage adds significantly to the output noise unless the available gain of the first stage $Gav_1 \gg F_2 - 1$. It is this requirement on first-stage gain that leads to the choice of the common-emitter configuration for the input stage. For each configuration, the source resistance for minimum noise factor is the same, and it is also approximately the source resistance for maximum power transfer for the common-emitter connection.[3] Thus, for the lowest noise and maximum power gain, one would choose the common-emitter connection.

3.3 Example of Sense Amplifier Design for Low Noise

In order to test smaller films, the input stage of the sense amplifier used in the Lincoln Laboratory magnetic film pulse tester[13] was modified in order to improve its output signal-to-noise ratio. The first-stage emitter current of the original amplifier (common-emitter) was 10 ma and the sense line resistance was 1.2 ohm, with the amplifier input direct coupled to the sense line. Referring to the noise figure graph of Fig. 8, we see that an amplifier with Rs $\approx$ 1

---

* Available gain = Gav = $\frac{\text{Power available at output}}{\text{Power available from source}}$

ohm and Ie = 10 ma has a noise figure approximately 20 db higher than the minimum due, primarily, to the small Rs. To reduce the noise figure to its minimum requires a transformed source impedance of the order of 1K indicating a transformer with a high step-up ratio (~ 1:30). The modification of the input stage included the insertion of a transformer of turns ratio 1:10 between sense line and input and the reduction of the input stage emitter current to 1 ma. Turns ratios higher than 1:10 resulted in signal pulse spreading due to transformer parasitics. With a turns ratio of 1:10 (Rs = 120) the noise figure at 1 ma is within 4 db of its minimum. The choice of the proper emitter current depends primarily on the necessity of providing the proper damping for the transformer. The above modification resulted in an output signal-to-noise ratio improvement of 16 db.

There is a practical point concerning the physical location of the transformer which is worth mentioning. Ordinarily, the sense amplifier input is connected to the sense line by means of a length of transmission line (e.g., twisted pair); for minimum signal attenuation, the transformer should be connected to the sense line side of the transmission line thereby placing the transmission line in the secondary (high impedance side) of the transformer. If the twisted pair is in the primary, the twisted pair inductance and transformer magnetizing inductance form an inductive voltage divider resulting in signal attenuation regardless of frequency.

4. THE FILTER-AMPLIFIER

4.1 The Readout Detection Problem

The magnetic film memory readout process consists essentially of determining the polarity of pulses due to flux rotation which occurs when the word driver is turned on. It is assumed that the time of occurrence of the pulses is known as well as the wave shape of the film switching pulse. The optimum design then consists in minimizing the probability of a false readout in the presence of noise given the wave shape and time of occurrence of the readout pulse. An idealized readout system is shown in Fig. 9. The block labelled S is an impulse sampler and decision element whose output assumes one of two possible levels depending on the value of v at the instant of sampling (t_1). The decision element may be idealized by giving it an infinitely sharp threshold. By impulse sampling we simply mean that the sampling pulse is very short compared with the signal pulse width. There are actually three random variables associated with the readout process. The first is the thermal and shot noise contributed by the amplifier and has normal statistics. The second is the signal amplitude A, which varies from element-to-element on a given sense line, and the third is the word noise amplitude W, which inevitably varies from word-to-word. The distributions of signal amplitude and word noise amplitude together with normal distribution of the shot and thermal noise may be used to determine the error

probability. We may, however, obtain an upper bound on the error probability by assuming that the signal amplitudes are all equal to the minimum and that the word noise is always the maximum. The effective signal amplitude A is than $A = A_{min} - W_{max}$. The mean square value of the noise will be denoted by σ^2.

Referring to Fig. 9, the voltage v(t) is the signal plus linearly-filtered shot and thermal noise. Fig. 10 shows the probability density of v(t) for equal bipolar pulses (1 and 0) of amplitude A with additive Gaussian noise. If equal weights are given to incorrect readouts of 1's and 0's, and the a priori probability of a 1 equals the a priori probability of a 0, the threshold of the decision element would be set at $v_o = 0$. The probability that noise will cause a false readout, i.e., $P(v < 0)$ for a 1, $P(v > 0)$ for a zero is then given by

$$P(v < 0)_1 = P(v > 0)_0 = P(\text{error}) = \int_{-\infty}^{0} p\,(v)\,dv = \int_{-\infty}^{0} \frac{e^{-(v - A)^2/2\sigma^2}}{\sqrt{2\pi}\,\sigma}\,dv$$

$$= \tfrac{1}{2}\left(1 - \operatorname{erf}\frac{A}{\sqrt{2}\sigma}\right) \qquad (29)$$

Minimization of the error probability is accomplished by maximizing the signal-to-noise ratio $(A/\sigma)^2$ at the output of the filter amplifier.

It is assumed implicitly that the memory cycle time, i.e., the time between successive readouts, is long compared with the correlation time of the filter amplifier so that each readout may be considered an independent event. Table I lists the error probability for increasing values of signal-to-noise ratio.[14] We are interested in very small error probabilities, i.e., the tail of the curve, because of the very high decision rates involved. For example, a 100-digit memory with a signal-to-noise ratio of 25 can expect a mean error-free time of only 0.035 second.

The mean time between failures for a one-digit system is $\left(\frac{1}{p}\right)\left(\frac{1}{f}\right)$ where p is the probability of error and f is the number of readouts per second (Appendix A). The mean time between failures for an m digit system is simply m times the MTBF for the one digit system (to a very good approximation. Appendix B). In Fig. 11 the mean time between failures is plotted as a function of $(A/\sigma)^2$ for hypothetical memories of 10 and 100 digits operating at (parallel) readout rates of 10^6 readouts/sec.

4.2 Maximizing Output Singla-to-Noise Ratio

4.2.1 The Matched Filter

In general, the problem of binary signal detection in the presence of noise involves deciding at the end of a time interval t_1 which one of two possible signals $e_1(t)$ or $e_2(t)$ has been sent. Since

TABLE I

A/σ	P(error)/digit	P(error)/100 digits	MTBF at 1 mc(sec)
4.0	3.0×10^{-5}	3.0×10^{-3}	3.3×10^{-4}
4.5	3.010	3.0×10^{-4}	3.3×10^{-3}
5.0	2.9×10^{-7}	2.9×10^{-5}	3.5×10^{-2}
5.5	2.2×10^{-8}	2.2×10^{-6}	4.5×10^{-1}
6.0	9.6×10^{-10}	9.6×10^{-8}	10
6.5	4.5×10^{-11}	4.5×10^{-9}	2.2×10^{2}
7.0	1.2×10^{-12}	1.2×10^{-10}	8.3×10^{3}
7.5	3.4×10^{-14}	3.4×10^{-12}	2.9×10^{5}

the probability of correct detection increases with increasing signal-to-noise ratio, defined as the square of the difference of the responses of the filter at $t = t_1$ to $e_1(t)$ and $e_2(t)$ divided by the mean square noise response, we wish to maximize that ratio. The linear time invariant filter interposed between noisy signal and detector which does this is called the matched filter, well known to radar receiver designers.[15, 16, 17] In general, the matched filter for $e_1(t)$ and $e_2(t)$ in white noise has the impulse response[17]

$$h(t) = e_1(t_1 - t) - e_2(t_1 - t) \ , \ 0 < t < t_1 \tag{30}$$

For our case of equal pulses of opposite phase, i.e., $e_1(t) = e_2(t) = e(t)$

$$h(t) = e(t_1 - t) \quad 0 < t < t_1 \tag{31}$$

that is, the optimum filter impulse response is the delayed mirror image of the input signal (Fig. 12). A very important result is that the signal-to-noise ratio at the output of the matched filter depends only on the ratio of input signal energy to input noise power per cycle. Specifically for our case (bipolar pulses)

$$(A/\sigma)^2 \,|_{\text{matched}} = \frac{8E}{N_o} \tag{32}$$

where E is the energy of a single pulse and $N_o/2$ is the input noise power density in watts/cps (double-sided spectrum). For the case where $e_2(t) = 0$, we have:

$$(A/\sigma)^2 \,|_{\text{matched}} = \frac{2E}{N_o} \tag{33}$$

that is, bipolar pulse transmission increases the signal-to-noise ratio four times. For a switched magnetic film, the total flux switched $\Phi = \int e \, dt$ is a fixed quantity invariant with respect to switching speed; the available energy of the switching pulse $\int \frac{e^2}{4 r_s} \, dt$, however, is proportional to switching speed. Thus, to increase signal-to-noise ratio, one must switch the film faster.

4.2.2 Single Time Constant Low Pass Filter with Rectangular Input Pulse

In this and the following two sections, we will determine the filter efficiency of three filter amplifier types for rectangular input pulses as a function of the filter parameters. The filter efficiency is defined as the signal-to-noise ratio at the output of the filter in question divided by the maximum signal-to-noise ratio attainable, i.e., the matched filter signal-to-noise ratio. For the filter amplifier considered in this and the following two sections, consider the block diagram of Fig. 13. In this diagram, the amplifier has been split into two parts; the first part is the first stage of the amplifier which is considered to be a (signal and noise) current source driving the remainder of the amplifier. In this sense, the remainder includes the first stage collector load (including the collector capacity). If we assume that the high-frequency cutoff of the entire amplifier is not determined primarily by the high frequency behavior of the current gain of the first stage,

then the frequency dependent transfer characteristics of the amplifier may be lumped into the remainder. The amplifier load has been chosen as 1 ohm so that mean square current and power are equal. For the low pass case, the current transfer function is:

$$G(j\omega) = G \frac{\omega_2}{\omega_2 + j\omega} \tag{34}$$

The noise output and signal transfer characteristics of the first stage are independent of frequency and may be considered fixed for the rest of the discussion. If the first stage noise power per cycle is $N_o/2$, the total noise power output of the entire amplifier is given by[18]

$$\sigma^2 = \frac{N_o^*}{2} \int_{-\infty}^{\infty} |\, G(j\omega) \,|^2 \, \frac{d\,\omega}{2\,\pi} = \frac{G^2\, N_o}{4\pi} \int_{-\infty}^{\infty} \frac{\omega_2^{\,2}}{\omega^2+\omega_2^{\,2}} \, d\,\omega \tag{35}$$

$$= \frac{G^2\, N_o\, \omega_2}{4}$$

We now calculate the maximum instantaneous signal power at the output of the filter. Consider a rectangular (signal) current pulse of length T and amplitude I applied to the remainder. The maximum output current is

$$A = IG\left(1 - e^{-\omega_2 T}\right) \tag{36}$$

---

* N_o is defined over positive frequencies so that $N_o/2$ is used in the integration over all frequencies.

$$\text{and } A^2 = I^2 G^2 \left(1 - e^{-\omega_2 T}\right)^2 \tag{37}$$

$$\text{so that } (A/\sigma)^2_{L.P.} = \frac{I^2}{N_o} \cdot \frac{4\left(1 - e^{-\omega_2 T}\right)^2}{\omega_2} \tag{38}$$

The matched filter output signal-to-noise ratio for the rectangular pulse is:

$$(A/\sigma)^2_{\text{matched}} = \left(\frac{2E}{N_o}\right) = \left(\frac{2I^2 T}{N_o}\right) \quad ** \tag{39}$$

Comparing equations 38 and 39, we have

$$\frac{(A/\sigma)^2_{L.P.}}{(A/\sigma)^2_{\text{matched}}} = \eta_{L.P.} = \frac{2\left(1 - e^{-\omega_2 T}\right)^2}{\omega_2 T} \tag{40}$$

Equation 40 has a maximum at $\omega_2 T \approx 1.3$. At this value of $\omega_2 T$ the signal-to-noise ratio for the single time constant low pass amplifier is about 25 per cent lower or 0.9 db lower than the matched filter signal-to-noise ratio. Equation 40 is plotted in Fig. 14 along with an experimentally-obtained curve. In the experiment a T2217 transistor (f_T = 900 mc, β = 100) was used as the input stage of a three-stage amplifier. The low pass cutoff frequency was determined by an RC network in the second-stage collector and was varied from 9 mc to 600 KC by changing the capacitance. The input pulse was rectangular with constant width. For each value of ω_2 the output pulse amplitude and noise power were measured.

** This is for an uni-polar signal. We will compute the various signal-to-noise ratios on the basis of uni-polar signals. The filter efficiencies thereby derived are the same as for bipolar signals.

4.2.3 Lumped Differentiating Filter-Amplifier

Consider a video amplifier where a single time constant high pass section has been introduced somewhere in the remainder to enable the amplifier to recover within one memory cycle from relatively low frequency transients. The low pass characteristic of the amplifier is assumed to be single time constant as in 4.2.2. The current transfer function of the remainder is:

$$G(j\omega) = G\left(\frac{\omega_2}{\omega_1 + j\omega}\right)\left(\frac{j\omega}{\omega_1 + j\omega}\right) \tag{41}$$

where the single time constant low pass factor with corner frequency ω_2 represents the low pass behavior of the original amplifier and the single time constant high pass factor with corner frequency ω_1 represents the differentiator. Since ω_2 may be greater or smaller than ω_1, neither frequency can be properly called the high or low frequency cutoff. We will show that introduction of the high pass "differentiator" results in a reduction of the output signal-to-noise ratio. The noise output of the amplifier is

$$\sigma^2 = \frac{N_o}{2}\int_{-\infty}^{\infty} |\, G\,(j\omega)\,|^2 \frac{d\,\omega}{2\,\pi} = G^2\,\frac{N_o}{4\pi}\int_{-\infty}^{\infty} \left|\, \frac{\omega_2\, j\omega}{(\omega_2 + j\omega)\,(\omega_1 + j\omega)}\,\right|^2 d\,\omega$$

$$= \frac{G^2\, N_o}{4} \cdot \frac{\omega_2^{\,2}}{(\omega_1 + \omega_2)} \qquad \text{(Bierens de Haan, p 47 \#7)} \tag{42}$$

As before, we consider a rectangular signal current pulse applied to the remainder and determine the maximum output amplitude. The result is:[19]

$$A^2 = I^2 G^2 \left(\frac{\omega_2}{\omega_2 - \omega_1}\right)^2 \left(e^{-\omega_1 t_M} - e^{-\omega_2 t_M}\right)^2 \qquad (43)$$

t_M is the time at which the maximum occurs. $t_M = \frac{1}{\omega_2 - \omega_1} \ln \frac{\omega_2}{\omega_1}$

Combining 42 and 43 we have

$$(A/\sigma)^2_{\text{lumped diff.}} = \frac{4I^2}{N_o} \frac{(\omega_1 + \omega_2)\left(e^{-\omega_1 t_M} - e^{-\omega_2 t_M}\right)^2}{(\omega_2 - \omega_1)^2} \qquad (44)$$

Comparing the lumped differentiator signal-to-noise ratio to the matched signal-to-noise ratio:

$$\frac{(A/\sigma)^2_{\text{lumped diff.}}}{(A/\sigma)^2_{\text{matched}}} = \eta = \frac{2(\omega_1 + \omega_2)\left(e^{-\omega_1 t_M} - e^{-\omega_2 t_M}\right)^2}{T(\omega_2 - \omega_1)^2} \qquad (45)$$

The inverse dependence of η on T reflects the fact that the differentiator utilizes only the portions of the signal energy near the pulse transitions whereas the matched filter (an integrator in this case) uses all the signal energy.

The efficiency of the lumped differentiator is shown as a function of $\frac{\omega_2}{\omega_1}$ with $\omega_2 T$ as a parameter for pulse widths greater than t_M,

the time at which maximum output occurs, in Fig. 15. The signal-to-noise ratio for a lumped differentiator-amplifier was determined experimentally as a function of $\frac{\omega_2}{\omega_1}$. The results are compared with the theoretical curve in Fig. 16. The amplifier used was the same as in 4.2.2. For this measurement ω_1 was established by shunting the third-stage collector resistor with inductors of varying values. The maximum output signal amplitude and noise powers were measured for each value of ω_1. During the experiment ω_2 was unchanged.

4.2.4 Distributed Element Differentiating Filter-Amplifier with Rectangular Input Pulse

Consider an amplifier where a distributed equivalent of the high pass section is inserted into the remainder for quick recovery purposes. The physical realization of such a network may take a number of forms, for example, a resistance shunted by a length of shorted transmission line has some of the properties of a parallel RL network. With such a network inserted into the remainder (if the resistance equals the characteristic impedance of the line) the current transfer function becomes

$$G(j\omega) = G\left(\frac{\omega_2}{\omega_2 + j\omega}\right)\left(\frac{1}{1 - j\ \mathrm{Ctg}\ \omega/\omega_1}\right) \quad \text{(Appendix C)} \quad (46)$$

where ω_1 is the reciprocal of the one-way propagation time for the line. The output noise power is

$$\sigma^2 = \frac{N_o}{2} \int_{-\infty}^{\infty} |\, G(j\omega)\, |^2 \frac{d\,\omega}{2\,\pi} = \frac{G^2\, N_o}{4\pi} \int_{-\infty}^{\infty} \frac{\omega_2^{\,2} \sin^2\left(\frac{\omega}{\omega_1}\right)}{\omega_2^2 + \omega^2}\, d\,\omega$$

$$= G^2\, N_o\, \frac{\omega_2}{8} \left(1 - e^{-2\,\omega_2/\omega_1}\right) \quad \text{(Bierens de Haan p 223 \#10)}$$

(47)

The maximum signal output for a rectangular input pulse is

$$A^2 = \left(\frac{G}{2}\right)^2 \left(1 - e^{-2\,\omega_2/\omega_1}\right)^2 I^2 \tag{48}$$

$$\text{So that } (A/\sigma)^2_{\text{dist. diff.}} = \frac{2\left(1 - e^{-2\,\omega_2/\omega_1}\right)}{\omega_2\, N_o}\, I^2 \tag{49}$$

Comparing 49 and 39

$$\frac{(A/\sigma)^2_{\text{dist. diff.}}}{(A/\sigma)^2_{\text{matched}}} = \eta = \frac{\left(1 - e^{-2\,\omega_2/\omega_1}\right)}{\omega_2\, T}\,, \quad T \geq \frac{2}{\omega_1} \tag{50}$$

A measurement similar to that in 4.2.3 was made for the distributed differentiator. In this case the inductors were replaced by shorted lengths of coaxial cable. Signal amplitude and noise measurements were made for varying lengths of cable. The experimental and theoretical curves are shown in Fig. 17.

4.2.5 Matched Filter for Memory Signals

In this section, we will discuss the relevance of the preceding results to film memory systems. We have used rectangular pulses as

input waveforms in the preceding calculations and experiments tacitly assuming that results obtained do not differ too greatly from those that would be obtained using a better approximation to the film switching voltage, e.g., triangular pulse, or gaussian pulse. In the following, we will attempt to demonstrate, without rigor, that this is the case. In Fig. 18 five pulse waveforms are shown together with the system functions of the corresponding matched filters. It is apparent that the first four waveshapes (uni-polar pulses) require similar filter characteristics for matching, i.e., low pass in contrast to the doublet pulse which requires a bandpass characteristic. The precise form of the film switching voltage will, or course, depend on the time variation of the driving field, however, it is safe to say that each pulse will be unipolar. The corresponding matched filter, whatever the details of the waveform, will therefore be low pass with bandwidth of the order of $\frac{1}{\text{Pulse Width}}$. The use of non-matched filter will, of course, result in the signal-to-noise ratio being slightly lower than the maximum attainable. We may estimate the penalty paid for using a non-matched low-pass filter of optimum bandwidth by referring to Table 2, which shows the loss in signal-to-noise ratio for some non-matched waveform-filter combinations.

4.2.6 Summary

To summarize, refer to Fig. 19 where we have traced the system signal-to-noise ratios through the transformations which result finally

TABLE 2[20]

Input Signal	Filter	Loss in $(A/\sigma)^2$ Compared with Matched Filter (db)
Rectangular	Gaussian	0.98
Gaussian	Ideal low pass	0.98
Rectangular	Rectangular	1.7
Rectangular	Single time constant low pass	0.88

in a mean time between failures for the system. The significant ratios are the available signal-to-noise ratio of the source $\int \frac{e^2 \, d\,t}{4\, r_s\, k\, T}$ (an energy ratio), the signal-to-noise ratio at the output of the first stage $8E/N_o$ (an energy ratio) and the signal-to-noise ratio at the output of the n-1 stage filter amplifier (a power ratio). The first two are related by the average noise factor $\overline{F}$ and the second two by the filter efficiency η . Relating the system parameters:

$$(A/\sigma)^2 = 8 \left(\frac{\int e^2 \, d\,t}{4\, r_s\, K\, T} \right) \left(\frac{1}{\overline{F}} \right) (\eta) \qquad (51)$$

We may note that for any film pulse $\int e^2 \, d\,t = \frac{C\, \Phi^2}{t_s}$ where Φ is the total switched flux, t_s is the switching time and C is a form factor which depends on the shape of the pulse (C = 1 for rectangular pulse, C = 4/3 for triangular pulse) so that in terms of total switched flux (for bipolar pulses)

$$(A/\sigma)^2 = \frac{2C\, \Phi^2\, \eta}{r_s\, k\, T\, t_s\, \overline{F}} \qquad (52)$$

At this point, it may be a good idea to review the approximations and assumptions that resulted in equation 52.

a. The effect of noise sources external to the memory system is small compared with internal (source resistance and amplifier) noise sources, i.e., the memory is adequately shielded.

b. The signal source impedance is adequately represented by a resistance of value r_s over the filter pass band.

c. The first stage gain is sufficiently high so that noise contributions from succeeding stages may be ignored.

d. The filter characteristic of the multistage amplifier is determined primarily by the n-1 stages following the first stage. In this respect, the first-to-second stage coupling network (including first stage collector capacity) may be considered part of the n-1 stage filter. This assumption leads to:

e. The first stage may be considered a wide band noise current source and distortionless amplifier.

With regard to the relation between $(A/\sigma)^2$ and MTBF we assume:

a. Strobe width $\ll \frac{1}{\text{Filter Bandwidth}}$

b. Memory Cycle time $\gg \frac{1}{\text{Filter Bandwidth}}$

As an example, we will calculate $(A/\sigma)^2$ for the FX-1 magnetic film memory. The parameters for that system are:

Φ = 2.8×10^{-11} volt-sec. (10 mil 1000 Å film)

t_s = 30×10^{-9} sec.

r_s = 1 ohm

$\overline{F}$ = 560 (27.5 db, see Fig. 8)

η $\simeq$ 0.15 (A differentiating sense amplifier was used)

C = 4/3 (assume a triangular film pulse)

Substituting these values in equation 52, we find $(A/\sigma)^2 = 2.48 \times 10^4$, a sufficiently high signal-to-noise ratio. However, if a film having 1/20 the switched flux were used and all other parameters were unchanged $(A/\sigma)^2$ would drop to 62 yielding a MTBF of 1700 hours for our 100-digit 1 MC system. A further decrease in $(A/\sigma)^2$ of only 33 per cent, would drop the MTBF to 2.5 minutes. The FX-1 sense amplifier may easily be modified to increase its signal-to-noise ratio. The noise factor may be reduced considerably by interposing a step-up transformer between sense line and input. In addition, the filter efficiency may be increased to 75-80 per cent by changing to a low pass configuration. With these changes reliable operation would be attainable with 1.4×10^{-12} volt/sec. spots.

APPENDIX A

MTBF FOR A ONE DIGIT SYSTEM IN TERMS OF ERROR PROBABILITY

Let p = probability of error on a given readout, then q = 1-p = probability of correct readout and $p\,q^{k-1}$ = probability of one error and k-1 correct readouts in a row. The mean number of intervals between error is then:

$$\mu = \sum_{k=1}^{\infty} k\,p\,q^{k-1} = p \sum_{k=1}^{\infty} k\,q^{k-1}$$

$$= \sum_{k=1}^{\infty} \frac{d}{dq}\, q^{k} = p \frac{d}{dq} \sum_{k=1}^{\infty} q^{k}$$

$$= p \frac{d}{dq} \frac{q}{1-q} = \frac{1}{p}$$

If the time between intervals (cycle time) is $\frac{1}{f}$ then MTBF = $\left(\frac{1}{p}\right)\left(\frac{1}{f}\right)$

APPENDIX B

MTBF FOR M DIGIT SYSTEM IN TERMS OF MTBF FOR ONE DIGIT SYSTEM

At a given parallel readout of m digits an error may happen in the following mutually exclusive ways: (1) a single error may occur — this can obviously occur in m different ways (2) a number of errors, say r errors may occur. The number of ways in which an r^{th} order error may occur is given by the binomial coefficient $\binom{m}{r} = \frac{m!}{r!\,(m-r)!}$ [14]. Since the errors on the individual digits are statistically independent, the probability of an r^{th} order error is simply p^r where p is the error probability for a single digit. To find the total error probability we sum over all possible r

$$p_{Total} = \sum_{r=1}^{m} \frac{m!}{r!(m-r)!} \cdot p^r$$

$$= m\,p + \underbrace{\sum_{r=2}^{m} \frac{m!}{r!(m-r)!}\, p^r}_{\text{multiple error contribution}}$$

For any realistically small value of p the second term is negligibly small compared with the single error term.

APPENDIX C

AN IMPEDANCE CALCULATION

The impedance of the parallel combination of a resistor Zo shunted by a length of transmission line (characteristic impedance = Zo, propagation time = T, termination impedance = Zr) measured at the resistor terminals is:

$$Z_{parallel} = \frac{Zo \cdot Z_{line}}{Zo + Z_{line}}$$

where

$$Z_{line} = Zo \frac{Zr + j\, Zo \tan \omega T}{Zo + j\, Zr \tan \omega T}$$ [21]

for Zr = 0 this becomes:

$$Z_{line} = Zo\, j \tan \omega T$$

so that

$$Z_{parallel} = \frac{Zo(Zo\, j \tan \omega T)}{Zo + j\, Zo \tan \omega T}$$

$$= \frac{Zo}{1 - j\, C\, tg\, \omega T}$$

REFERENCES

1. T. Crowther, "High Density Magnetic Film Memory Techniques" 1964 Proc. Intermag Conf.

2. J. I. Raffel, "Future Developments in Large Magnetic Film Memories," Proc. Ninth Symposium on Magnetism and Magnetic Materials, Journal of Applied Physics.

3. E. G. Nielsen, "Behavior of Noise Figure in Junction Transistors," Proc. IRE, 45, p 957, (July 1957).

4. R. N. Beatie, "A Lumped Model Analysis of Noise in Semiconductor Devices," Trans. IRE PGED, pp 133, (April 1959).

5. W. Gugenbuehl and M. J. O. Strutt, "Theory and Experiments on Shot Noise in Semiconductor Junction Diodes and Transistors," Proc. IRE, 45, p 839, (June 1957).

6. D. G. Peterson, "Noise Performance of Transistors," Trans. IRE PGED, p 296, (May 1962).

7. G. H. Hanson and A. van der Ziel, "Shot Noise in Transistors" Proc. IRE, 45, p 1538, (November 1957).

8. J. I. Raffel, et. al., "Magnetic Film Memory Design," Proc. IRE, 49, p 155, (January 1961).

9. J. I. Raffel, et. al., "The FX-1 Magnetic Film Memory," Lincoln Laboratory Technical Report No. 278, (August 1962).

10. IRE Standards on Methods of Measuring Noise in Linear Twoports, Proc. IRE, (January 1960), 48, p 60.

11. H. A. Haus, et. al., "Representation of Noise in Linear Twoports" Proc. IRE, 48, p 69, (January 1960).

12. W. R. Bennett, Electrical Noise, McGraw-Hill, (1960).

13. A. H. Anderson and T. S. Crowther, "Techniques for Pulse Testing Magnetic Film Memory Elements," Lincoln Laboratory Group Report No. 51-11, (January 1960).

14. Feller, An Introduction to Probability Theory and its Applications, John Wiley and Sons, (1957).

15. G. L. Turin, "An Introduction to Matched Filters," Trans. IRE, PGIT IT-6, 311, (1960).

16. P. E. Green, Jr., "Radar Astronomy Measurement Techniques" Lincoln Laboratory Technical Report No. 282.

17. E. J. Baghdady, Lectures on Communication System Theory, McGraw-Hill,(1961), Article by W. M. Siebert.

18. Y. W. Lee, Statistical Theory of Communication, John Wiley and Sons, (1960).

19. J. Millman and H. Taub, Pulse and Digital Circuits, McGraw-Hill (1959).

20. M. I. Skolnik, Introduction to Radar Systems, McGraw-Hill (1962).

21. W. C. Johnson, Transmission Lines and Networks, McGraw-Hill (1950).

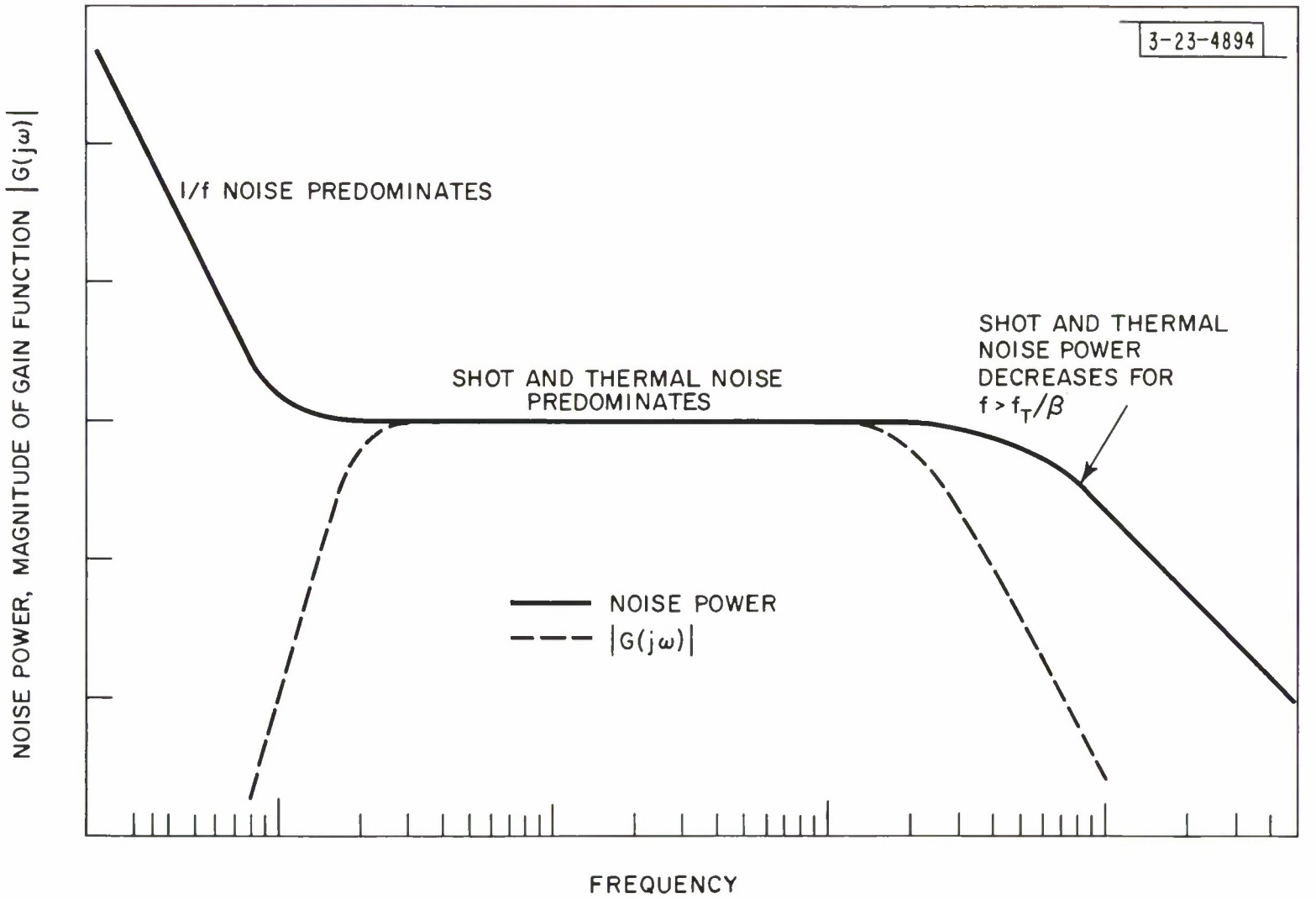

Fig. 1 First stage noise power spectrum and magnitude of gain function $|G(j\omega)|$ of remainder of amplifier.

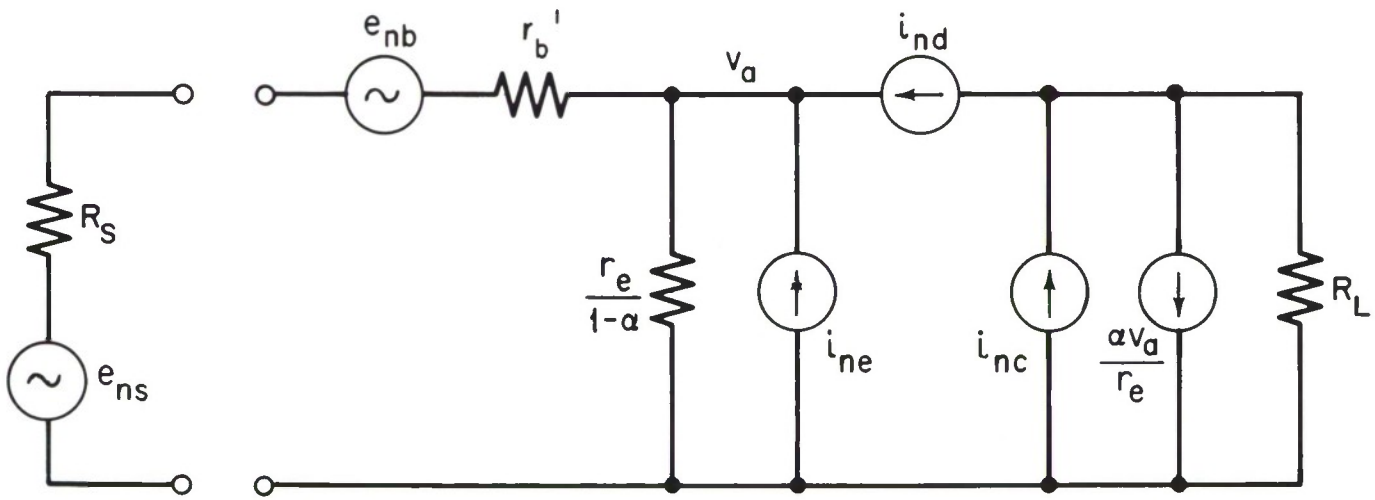

Fig. 2 Common emitter equivalent with superimposed noise sources.

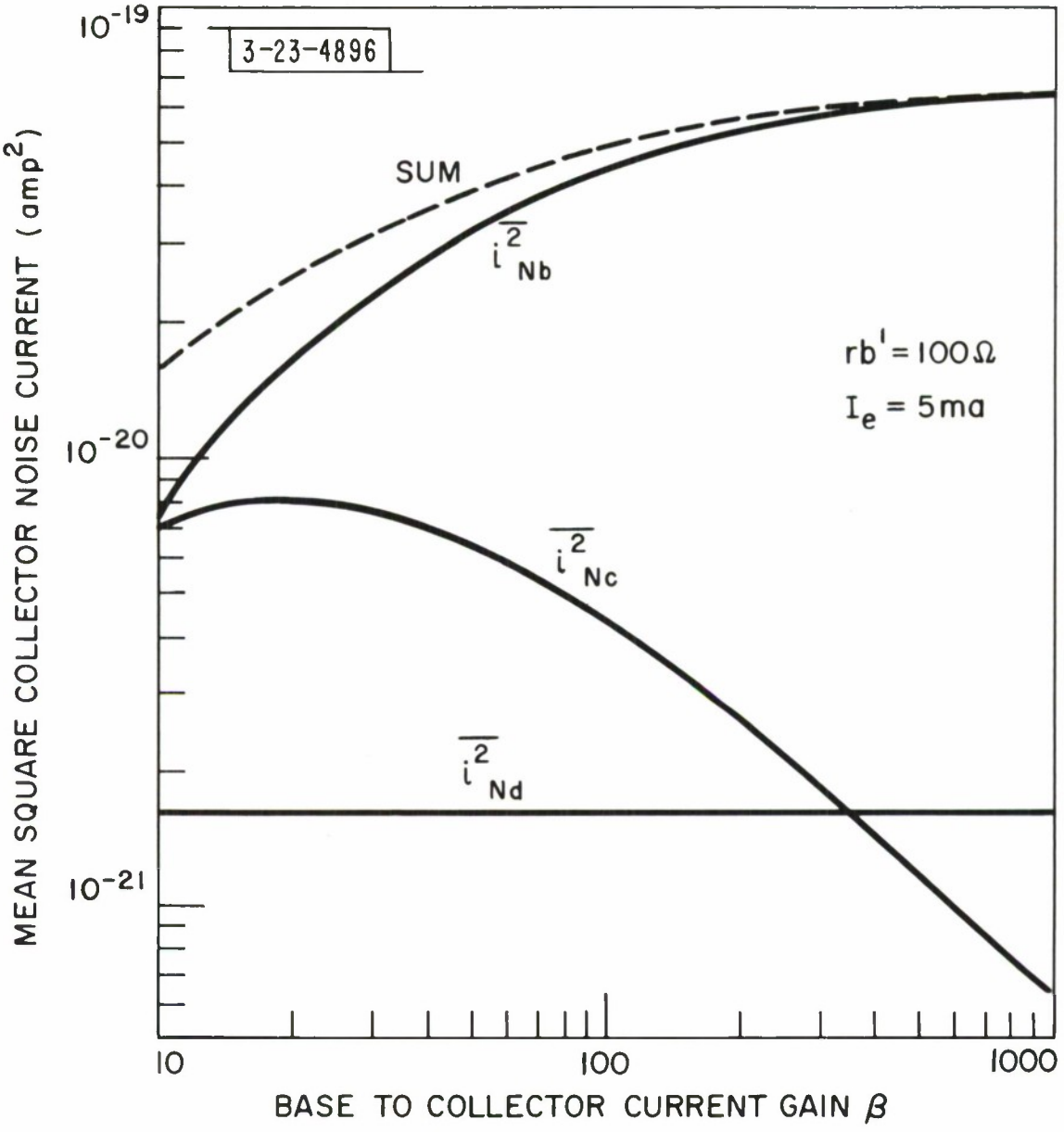

Fig. 3 Calculated mean square collector noise current as a function of current gain β for common emitter with $R_s = 0$.

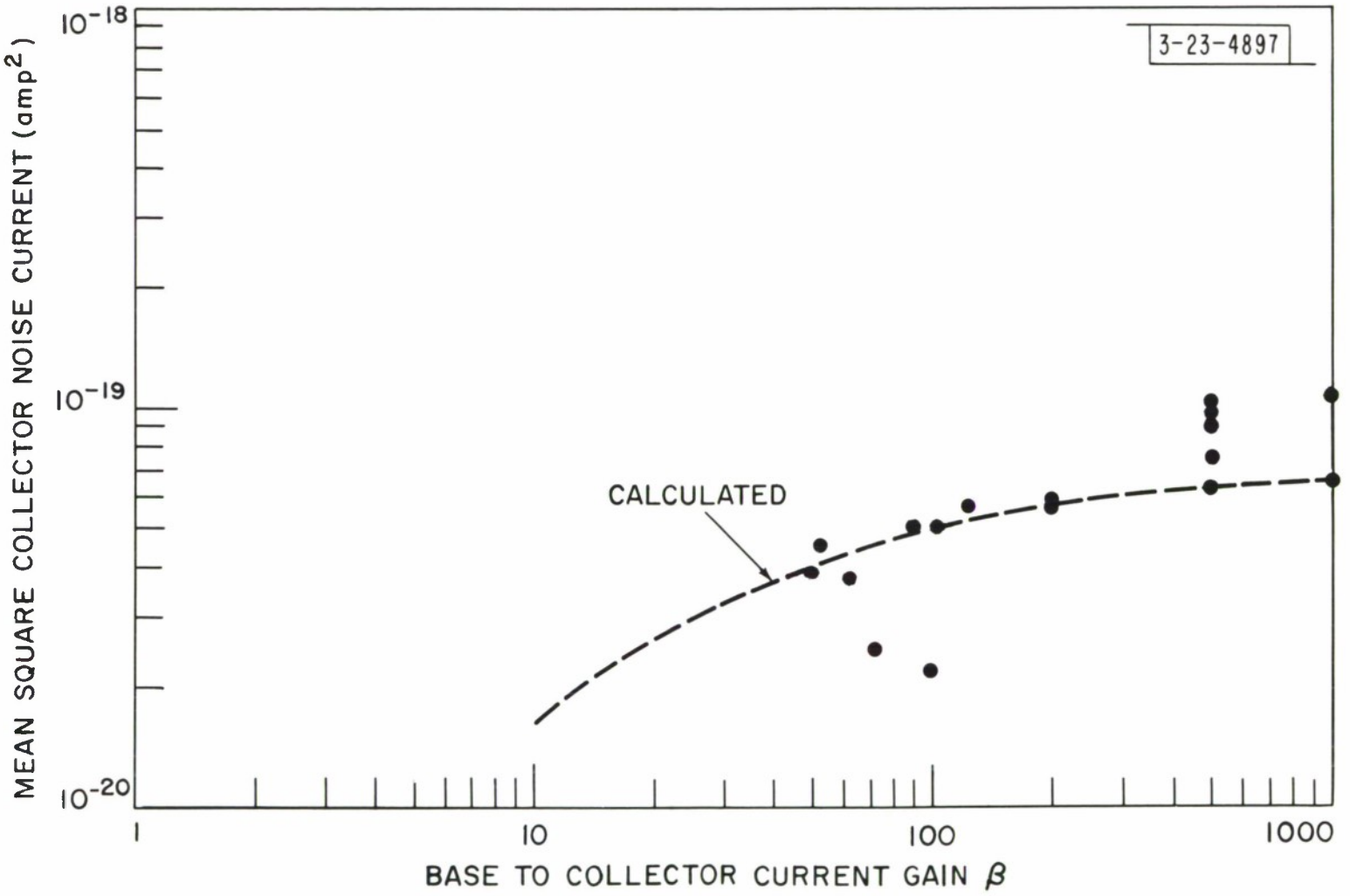

Fig. 4 Mean square collector noise current for 18 T2217 transistors with different current gains β, as a function of β. Common emitter; $R_s = 0$.

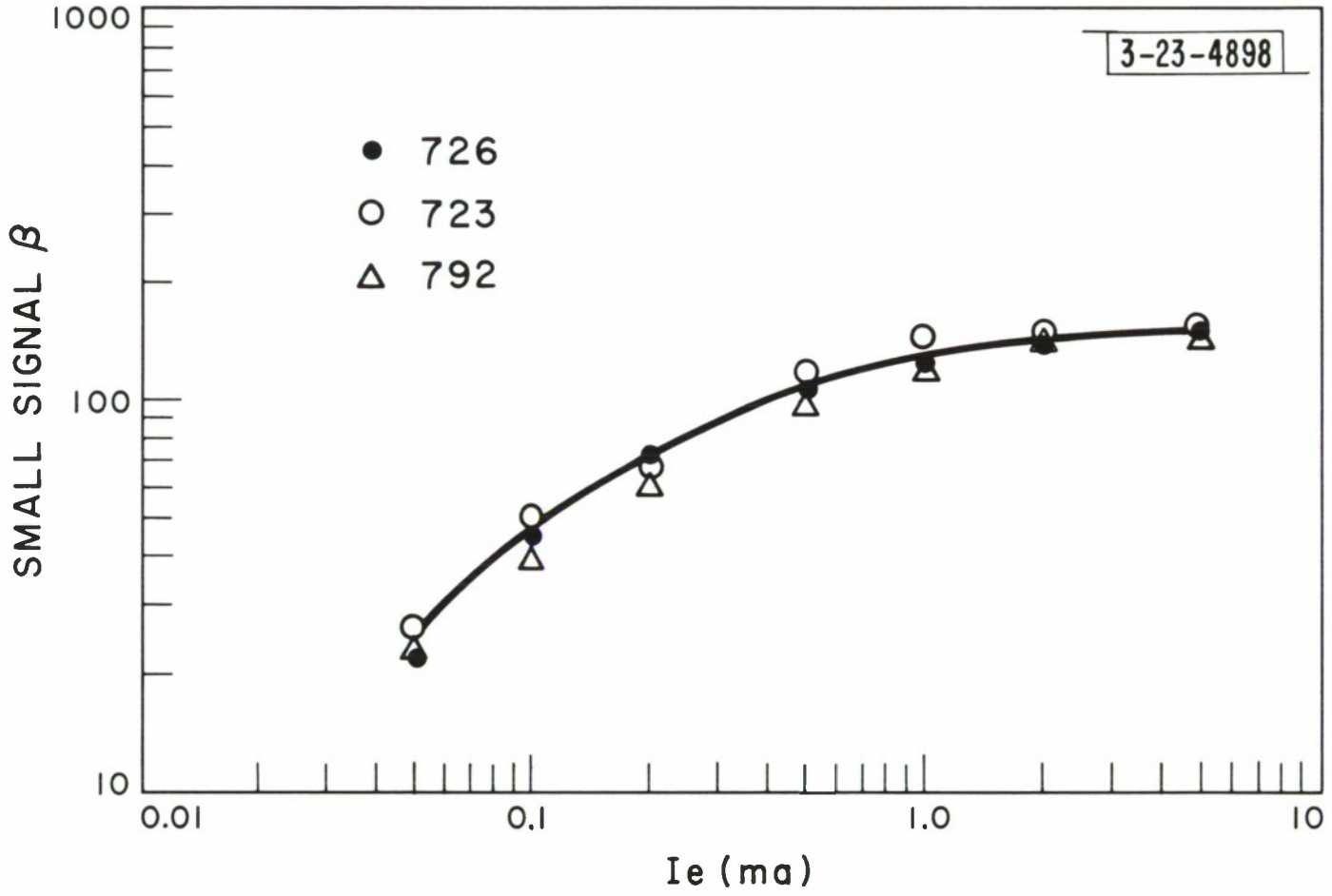

Fig. 5 Current gain β as a function of emitter current for 3 T2217 transistors.

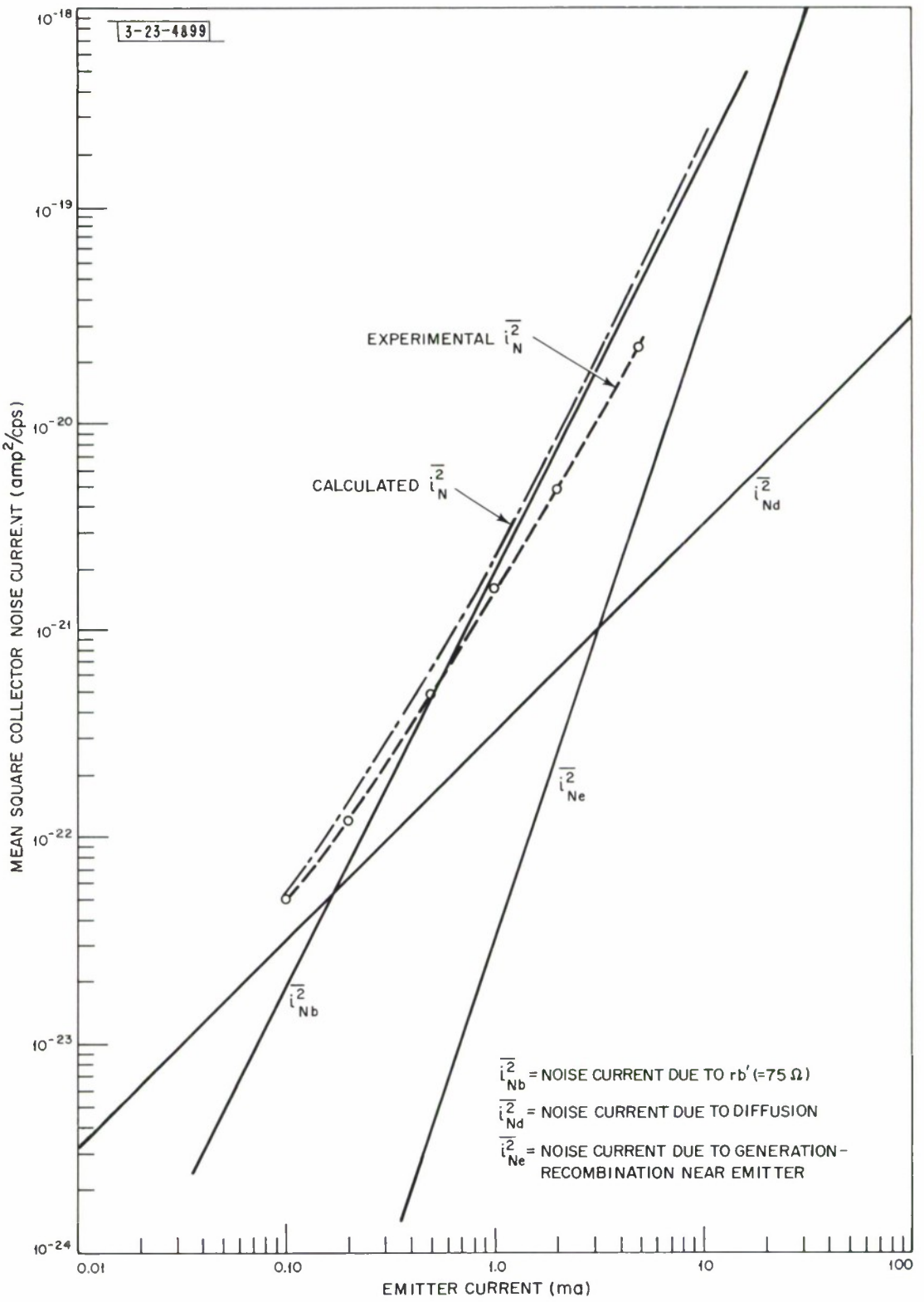

Fig. 6 Collector noise current components as function of emitter current calculated using Beatie — Peterson model compared with experimentally obtained curve. Common emitter connection with $R_s = 0$.

3-23-4900

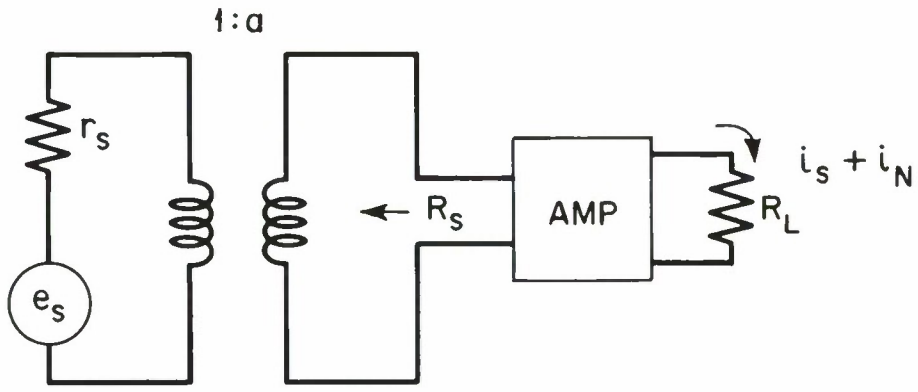

Fig. 7 Amplifier input network.

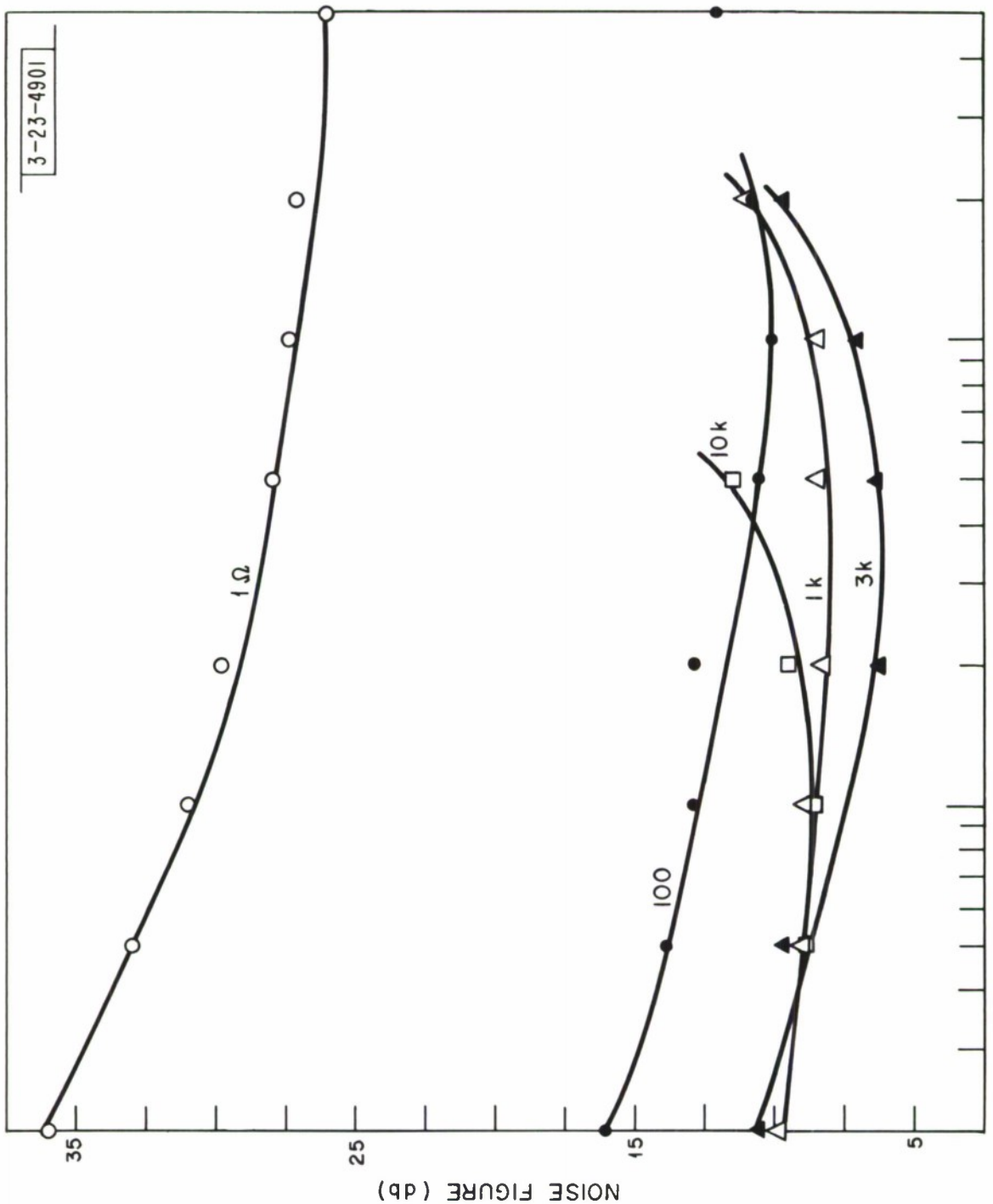

Fig. 8 Average noise figure as function of emitter current with source resistance R_s as parameter.

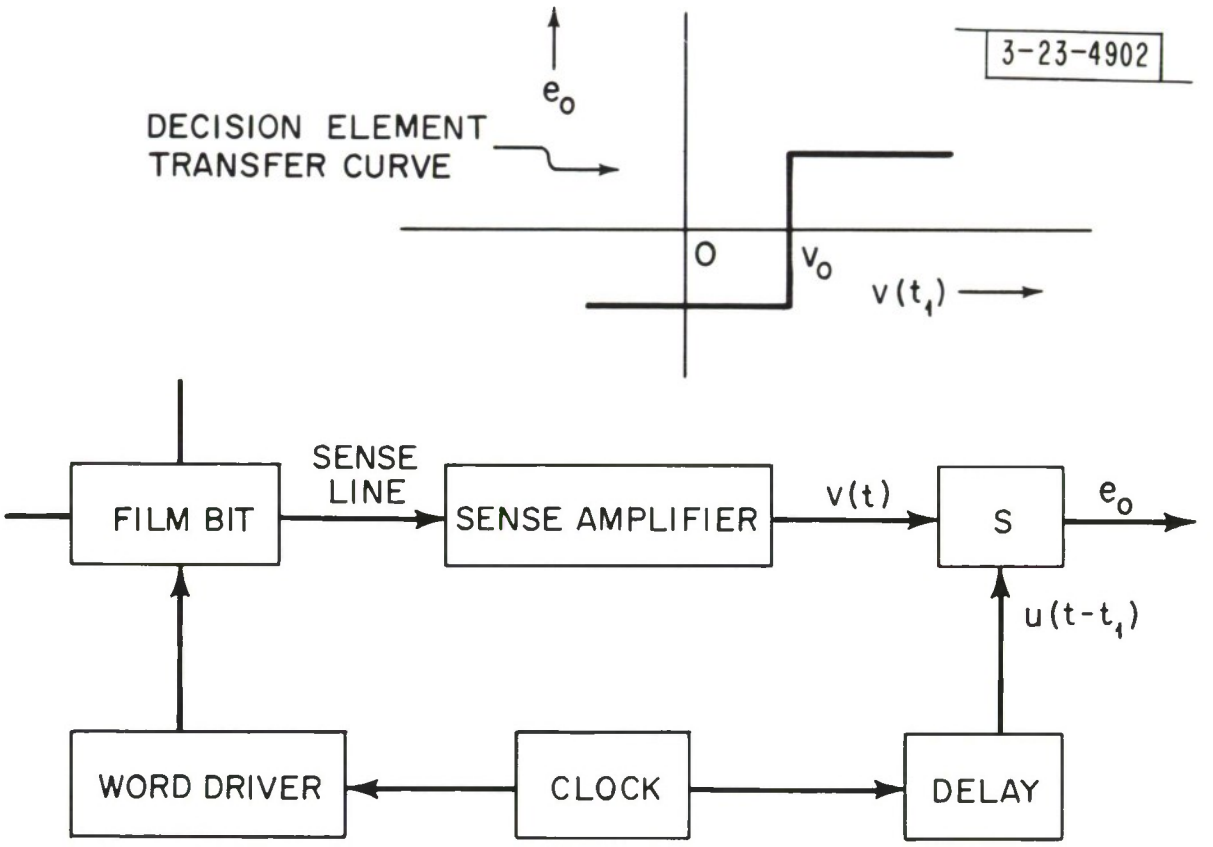

Fig. 9 Block diagram of readout system.

3-23-4903

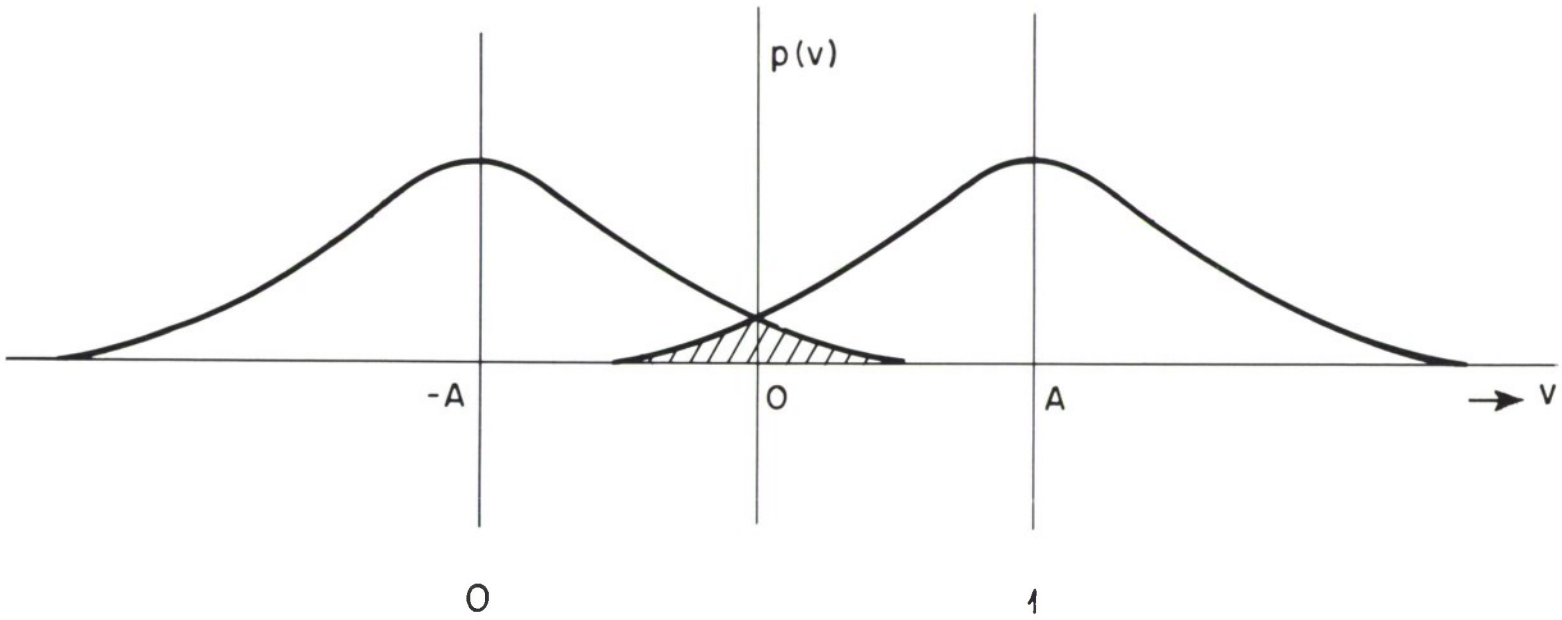

Fig. 10 Probability density of detector input v (t) for bipolar signals and additive Gaussian noise.

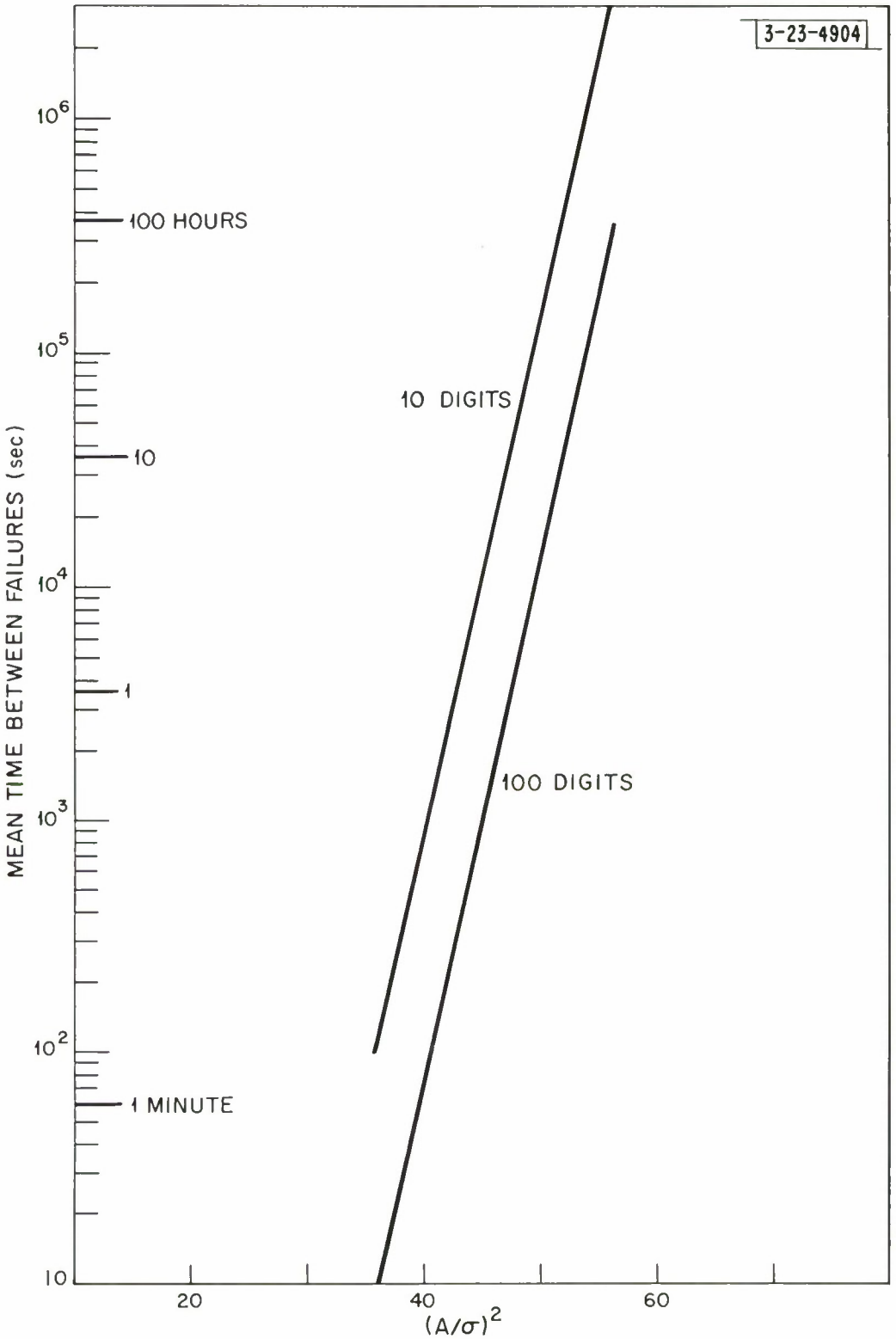

Fig. 11 Mean time between failures as function of output signal-to-noise ratio $(A/\sigma)^2$ for 1 mc readout rate.

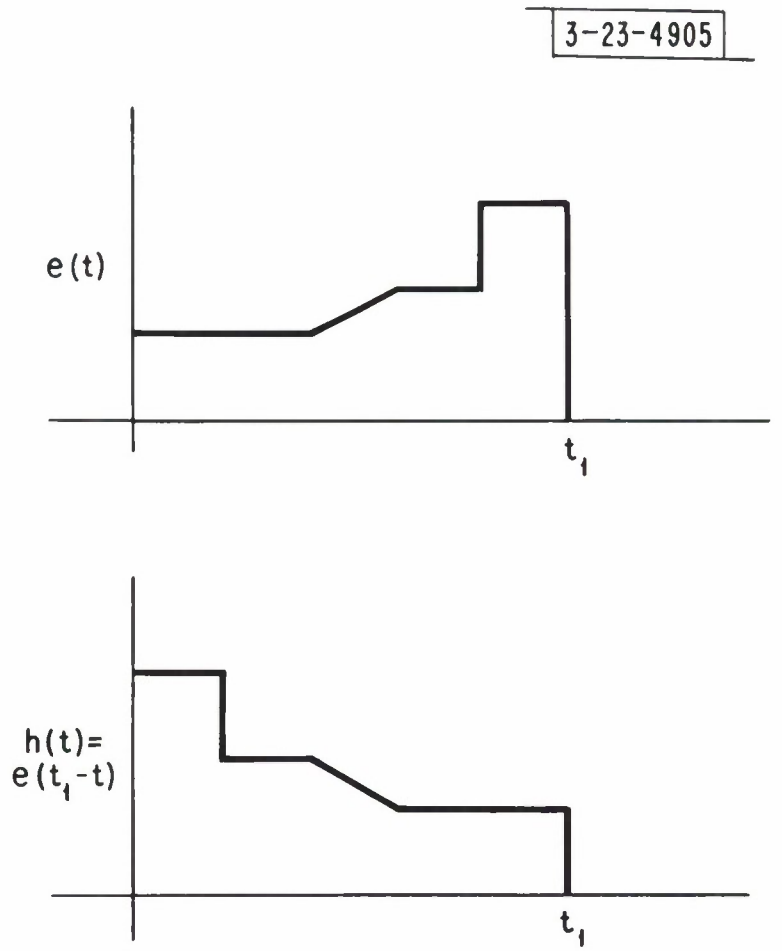

Fig. 12 A signal waveform and a matched filter impulse response.

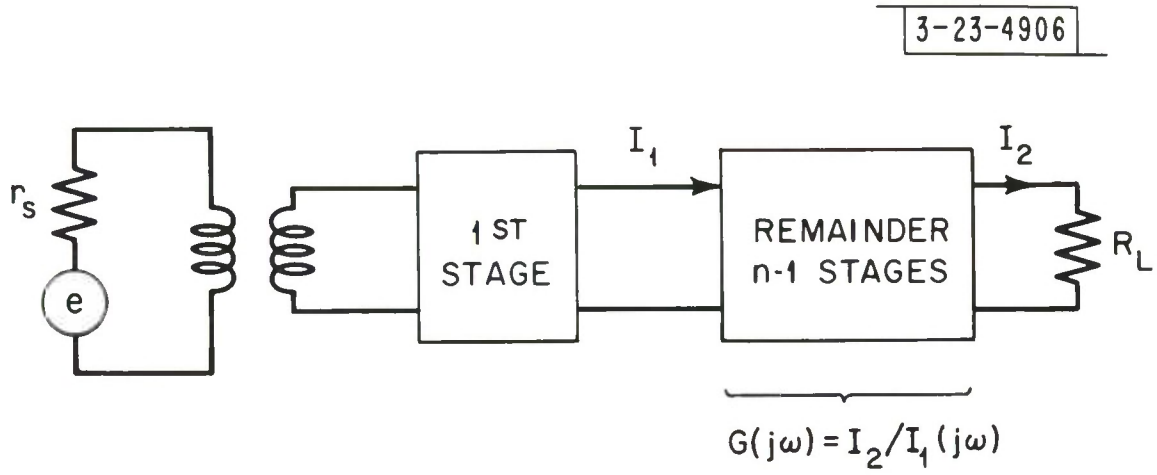

Fig. 13 Block diagram of n-stage sense amplifier.

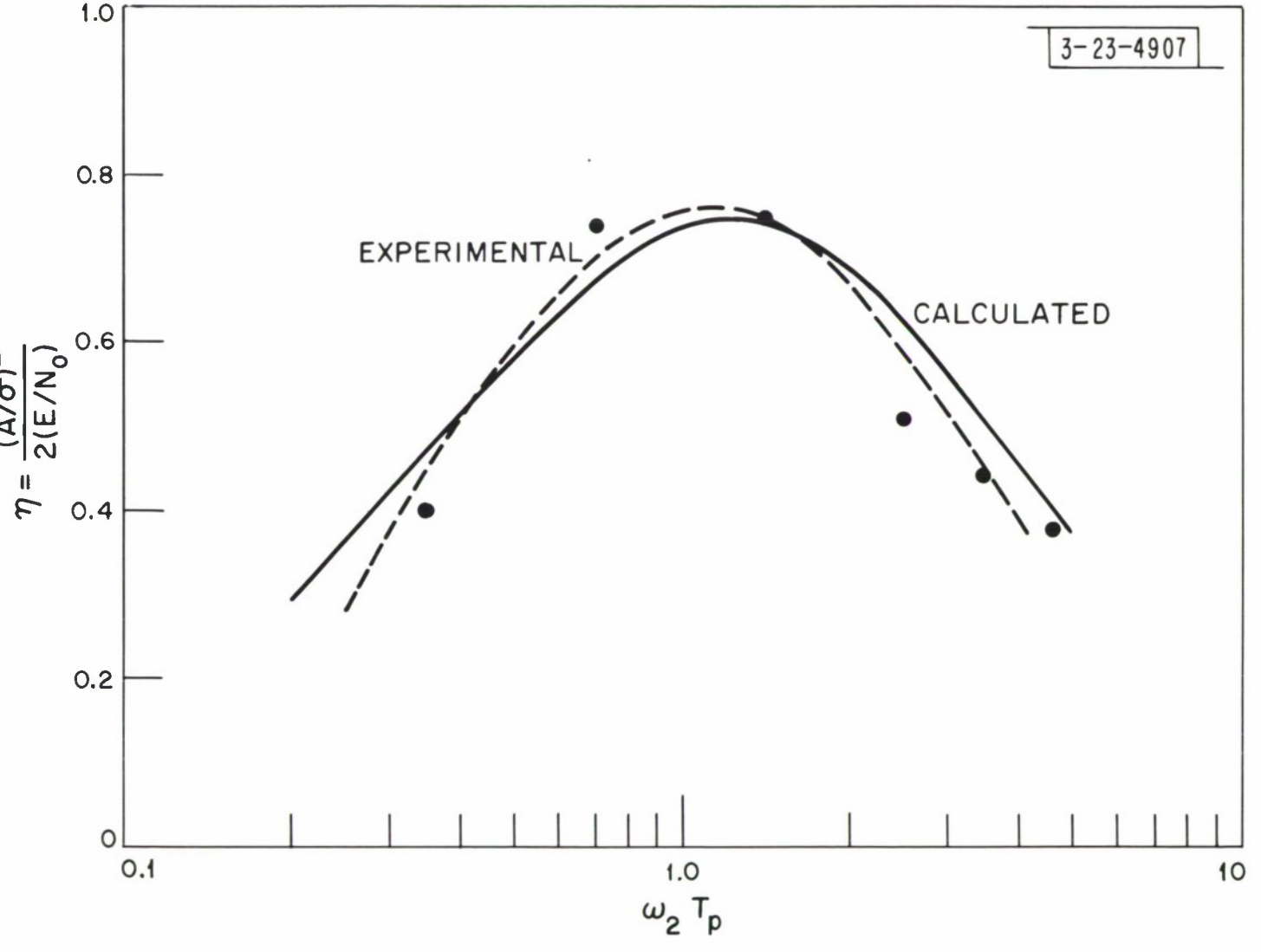

Fig. 14 Efficiency of single time constant low pass filter for rectangular pulse in white noise.

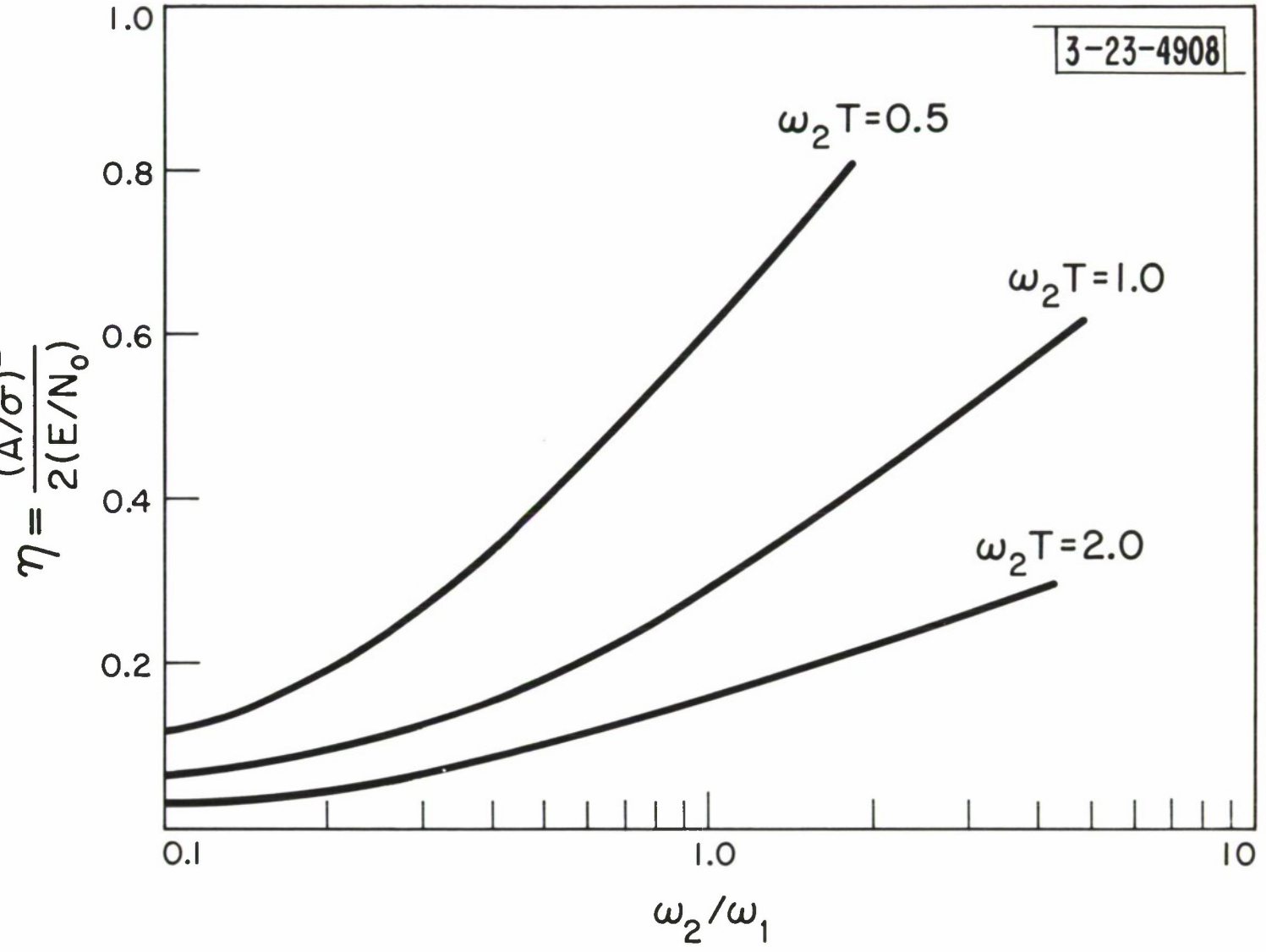

Fig. 15 Theoretical efficiency of lumped differentiator for rectangular pulse in white noise with $\omega_2 T$ as parameter.

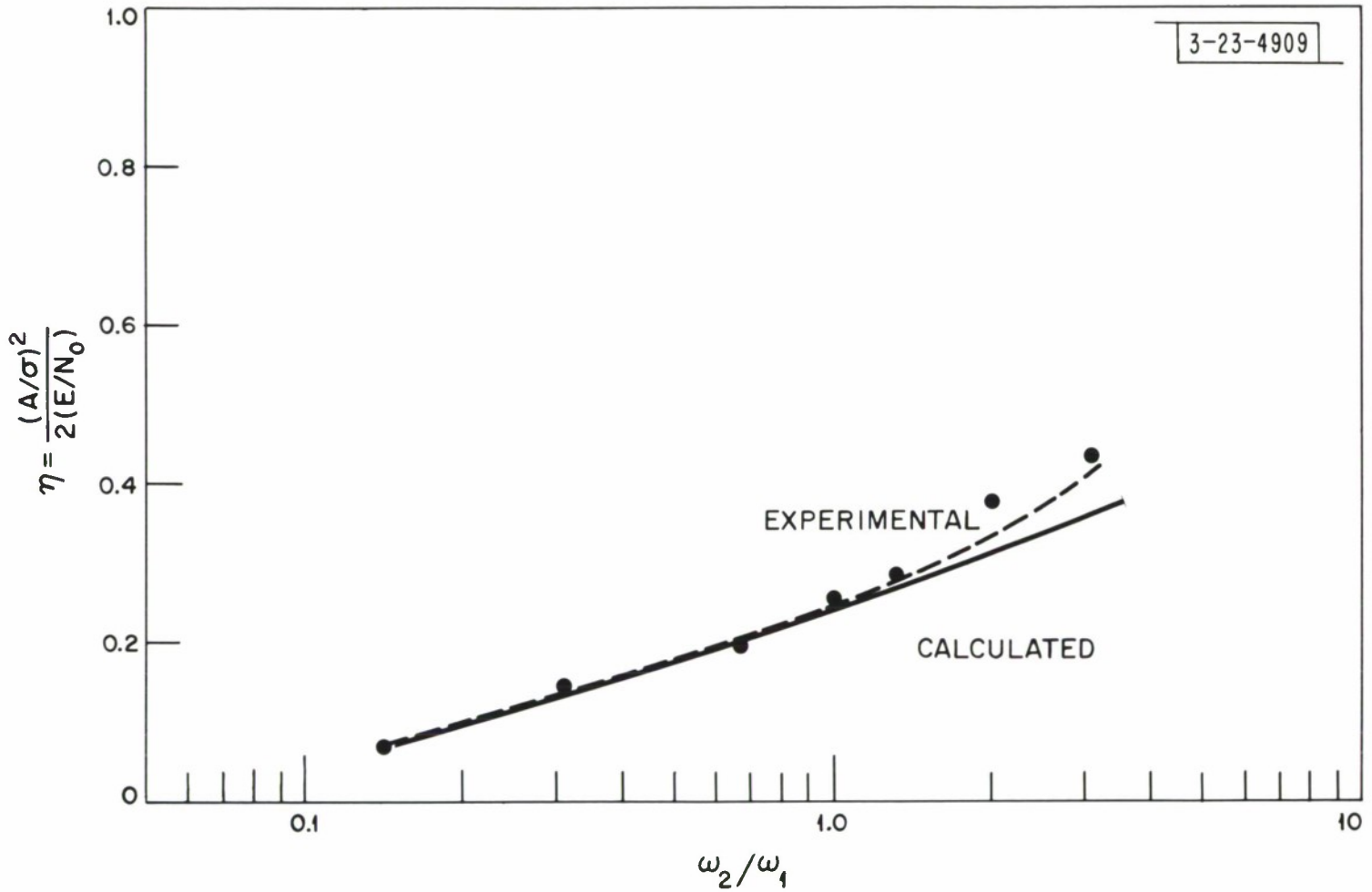

Fig. 16 Efficiency of lumped differentiator for rectangular pulse in white noise; $\omega_2 T = 1.6$.

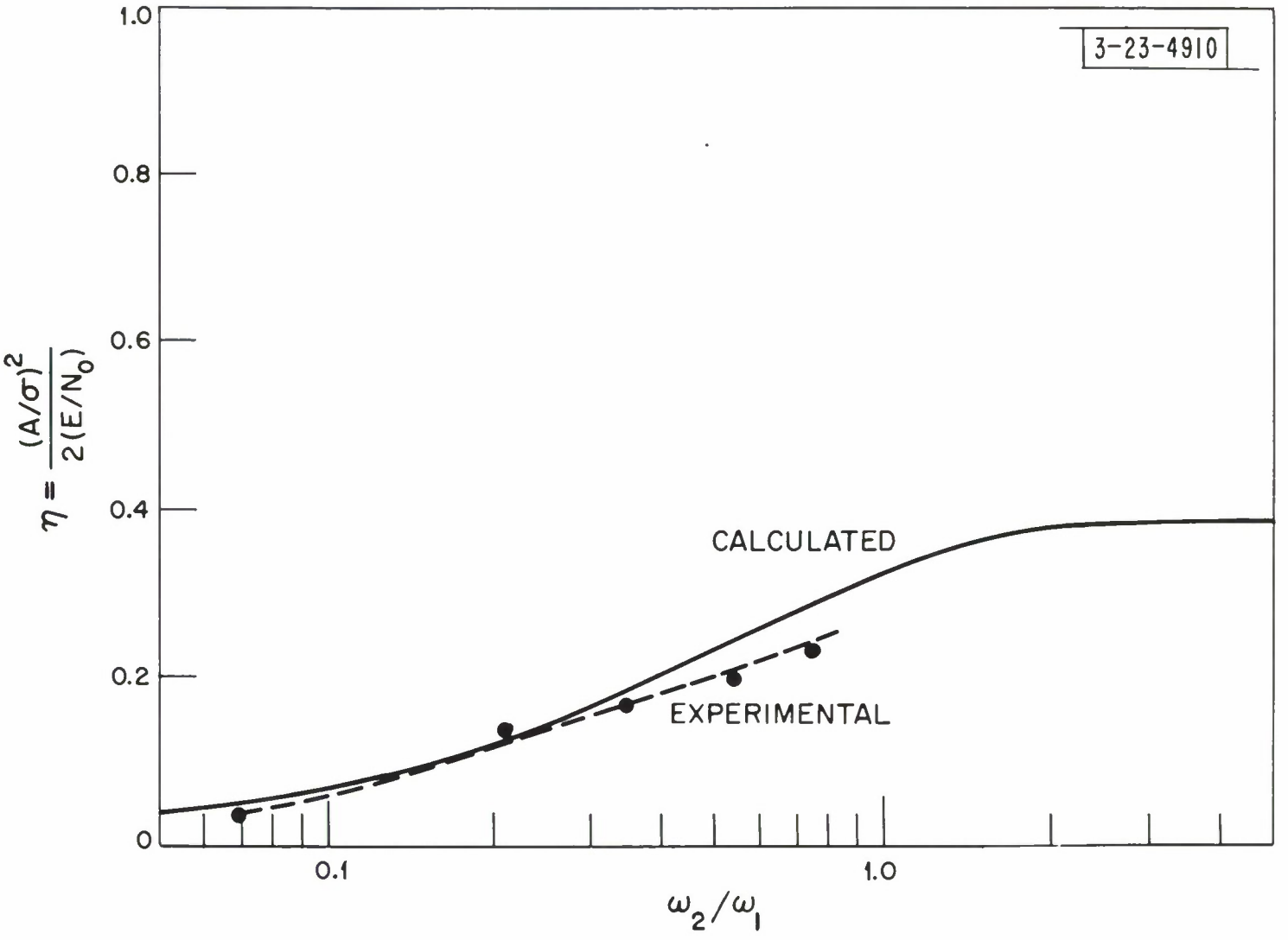

Fig. 17 Efficiency of distributed differentiator for rectangular pulse in white noise; $\omega_2 T = 2.5$.

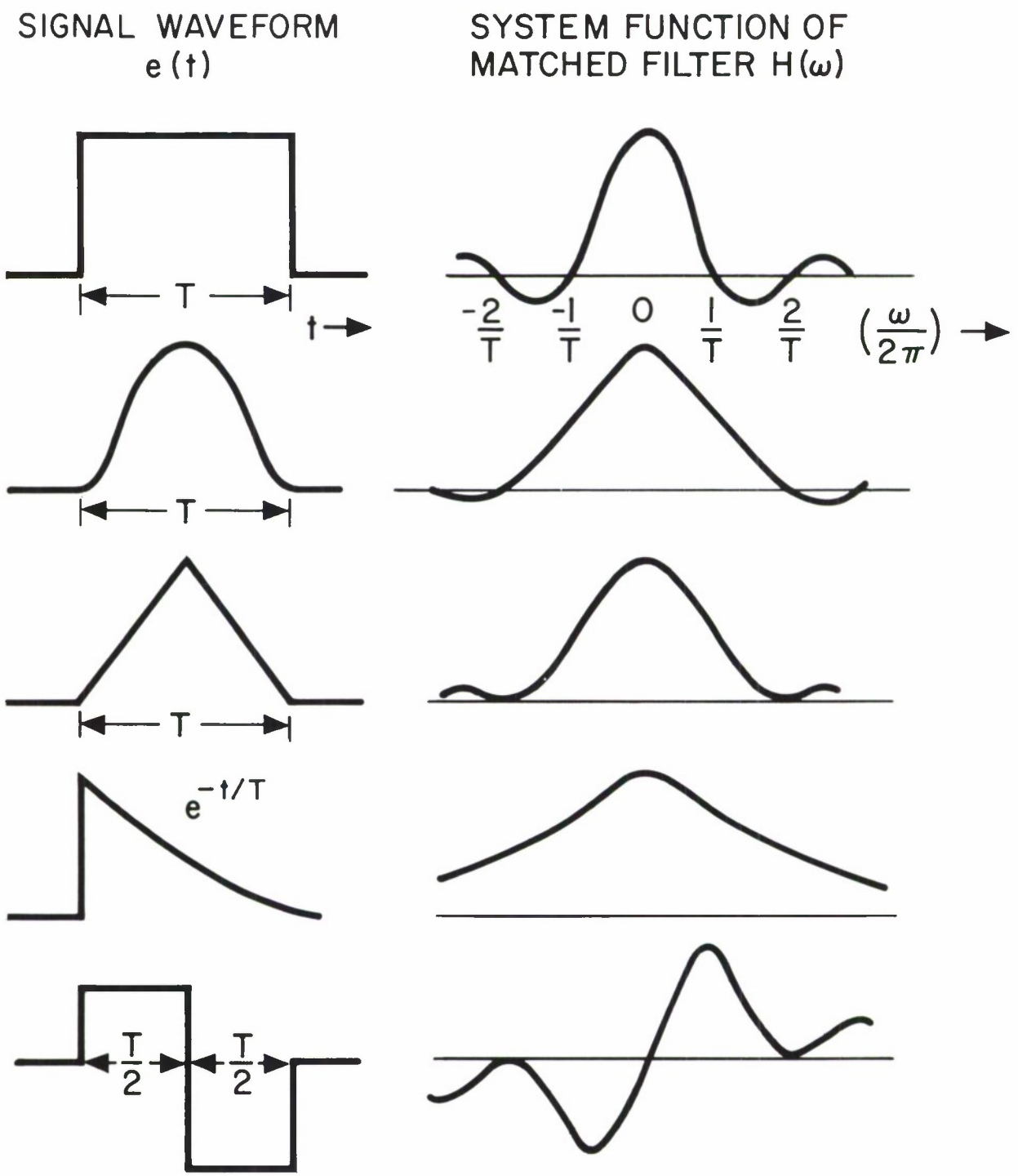

Fig. 18 Some pulse waveforms and the corresponding matched filters.

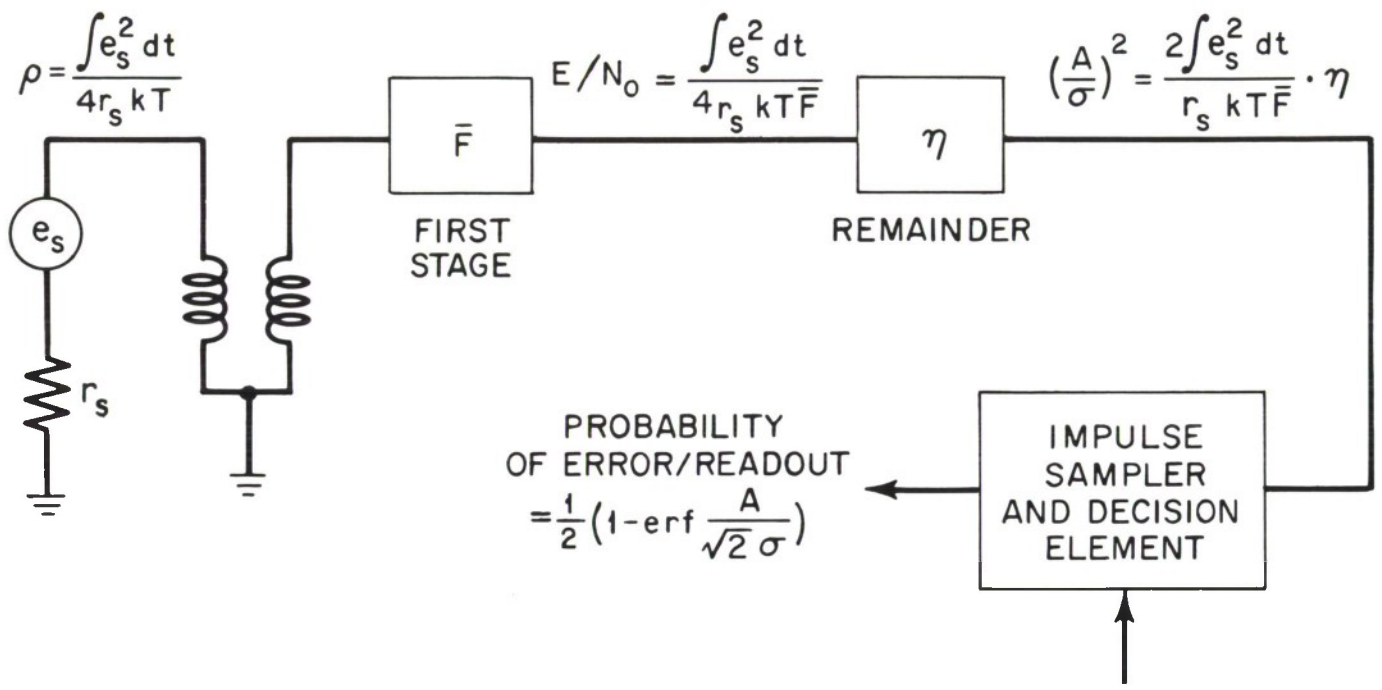

Fig. 19 Block diagram of sense amplifier showing signal-to-noise ratio transformations.

DISTRIBUTION LIST

Division 2

F. C. Frick

Group 21

R. M. Horowitz

Group 24

R. C. Johnson

C. T. Kirk

Group 23

A. H. Anderson

P. E. Barck

H. Blatt (50 copies)

R. L. Burke

N. Colher

S. M. Cotton (5 copies)

T. S. Crowther

D. J. Eckl

J. Feldman

C. Forgie

J. M. Frankovich

G. P. Gagnon

E. A. Guditz

J. Heart

Group 23 Continued

T. O. Herndon

C. A. Hoover

R. W. Hudson

W. Kantrowitz

K. H. Konkle

J. E. Laynor

C. S. Lin

J. J. Lynch

D. Malpass

W. J. Meyers

J. L. Mitchell

M. Naiman

C. A. Norman

S. Pezaris

J. D. Piro

J. I. Raffel

L. G. Roberts

D. O. Slutz

T. Stockham

W. R. Sutherland

A. Vanderburgh

O. C. Wheeler

C. Woodward

F. Vecchia

14. KEY WORDS	LINK A		LINK B		LINK C	
	ROLE	WT	ROLE	WT	ROLE	WT
Data Processing Memory Unit Magnetic Film Noise Sensing System Signal Noise Ratio Amplifier Design						

INSTRUCTIONS

1. ORIGINATING ACTIVITY: Enter the name and address of the contractor, subcontractor, grantee, Department of Defense activity or other organization *(corporate author)* issuing the report.

2a. REPORT SECURITY CLASSIFICATION: Enter the overall security classification of the report. Indicate whether "Restricted Data" is included. Marking is to be in accordance with appropriate security regulations.

2*b*. GROUP: Automatic downgrading is specified in DoD Directive 5200.10 and Armed Forces Industrial Manual. Enter the group number. Also, when applicable, show that optional markings have been used for Group 3 and Group 4 as authorized.

3. REPORT TITLE: Enter the complete report title in all capital letters. Titles in all casea should be unclassified. If a meaningful title cannot be selected without classification, show title classification in all capitals in parenthesis immediately following the title.

4. DESCRIPTIVE NOTES: If appropriate, enter the type of report, e.g., interim, progress, summary, annual, or final. Give the inclusive dates when a specific reporting period is covered.

5. AUTHOR(S): Enter the name(s) of author(s) as shown on or in the report. Enter last name, first name, middle initial. If military, show rank and branch of service. The name of the principal author is an absolute minimum requirement.

6. REPORT DATE: Enter the date of the report as day, month, year, or month, year. If more than one date appears on the report, uae date of publication.

7a. TOTAL NUMBER OF PAGES: The total page count should follow normal pagination procedures, i.e., enter the number of pages containing information.

7*b*. NUMBER OF REFERENCES: Enter the total number of references cited in the report.

8*a*. CONTRACT OR GRANT NUMBER: If appropriate, enter the applicable number of the contract or grant under which the report was written.

8*b*, 8*c*, & 8*d*. PROJECT NUMBER: Enter the appropriate military department identification, such as project number, subproject number, system numbers, task number, etc.

9a. ORIGINATOR'S REPORT NUMBER(S): Enter the official report number by which the document will be identified and controlled by the originating activity. This number must be unique to this report.

9*b*. OTHER REPORT NUMBER(S): If the report has been assigned any other repcrt numbers *(either by the originator or by the sponsor)*, also enter this number(s).

10. AVAILABILITY/LIMITATION NOTICES: Enter any limitations on further dissemination of the report, other than those imposed by security classification, using standard statementa such as:

(1) "Qualified requesters may obtain copies of this report from DDC."

(2) "Foreign announcement and dissemination of this report by DDC is not authorized."

(3) "U. S. Government agencies may obtain copies of this report directly from DDC. Other qualified DDC users ahall request through

_____."

(4) "U. S. military agencies may obtain copies of this report directly from DDC. Other qualified users shall request through

_____."

(5) "All distribution of this report is controlled. Qualified DDC users shall request through

_____."

If the report has been furnished to the Office of Technical Services, Department of Commerce, for aale to the public, Indicate this fact and enter the price, if known.

11. SUPPLEMENTARY NOTES: Use for additional explanatory notes.

12. SPONSORING MILITARY ACTIVITY: Enter the name of the departmental project office or laboratory sponsoring *(paying for)* the research and development. Include address.

13. ABSTRACT: Enter an abstract giving a brief and factual summary of the document indicative of the report, even though it may also appear elsewhere in the body of the technical report. If additional space is required, a continuation sheet shall be attached.

It is highly desirable that the abstract of classified reports be unclassified. Each paragraph of the abstract shall end with an indication of the military security classification of the information in the paragraph, represented as *(TS)*, *(S)*, *(C)*, or *(U)*.

There is no limitation on the length of the abstract. However, the suggested length is from 150 to 225 words.

14. KEY WORDS: Key words are technically meaningful terms or short phrases that characterize a report and may be used as index entries for cataloging the report. Key words must be selected so that no security classification is required. Identifiers, such as equipment model designation, trade name, military project code name, geographic location, may be used as key words but will be followed by an indication of technical context. The assignment of links, rules, and weights is optional.

UNCLASSIFIED
Security Classification

DOCUMENT CONTROL DATA - R&D

(Security classification of title, body of abstract and indexing annotation must be entered when the overall report is classified)

1. ORIGINATING ACTIVITY *(Corporate author)*: Lincoln Labs., Lexington, Mass.

2a. REPORT SECURITY CLASSIFICATION: UNCLASSIFIED

2b. GROUP: N/A

3. REPORT TITLE: Random Noise Considerations in the Design of Magnetic Film Sense Amplifiers

4. DESCRIPTIVE NOTES *(Type of report and inclusive dates)*: Group Report

5. AUTHOR(S) *(Last name, first name, initial)*: Blatt, H.

6. REPORT DATE	7a. TOTAL NO. OF PAGES	7b. NO. OF REFS
Aug 64	62	0

8a. CONTRACT OR GRANT NO.	9a. ORIGINATOR'S REPORT NUMBER(S)
AF19(628)500	GR-1964-6
b. PROJECT NO.	
c.	9b. OTHER REPORT NO(S) *(Any other numbers that may be assigned this report)*
d.	ESD-TDR-64-365

10. AVAILABILITY/LIMITATION NOTICES: Qualified Requesters May Obtain Copies From DDC.

11. SUPPLEMENTARY NOTES	12. SPONSORING MILITARY ACTIVITY
	ESD. L.G. Hanscom Field, Bedford, Mass.

13. ABSTRACT

A model of a magnetic film sense system is presented. Using the model the mean time between false readouts due to random noise is determined as a function of the system parameters; total magnetic flux switched, switching time, sense line resistance, amplifier noise factor and linear amplifier efficiency. (The filter efficiency with respect to a given input pulse shape is the signal-to-noise ratio at the output of the amplifier divided by the corresponding signal-to-noise ratio at the output of a filter matched to the pulse shape.) The degradation of signal-to-noise ratio caused by introduction of a quick recovery "short" time constant is determined and shown experimentally.

DD FORM 1 JAN 64 1473

Security Classification
UNCLASSIFIED